が明らかになっている。このとき腎におけるカルビンディン D_{9K} の発現が低下しており，カルシウム再吸収過程に関与していると考えられる。一方でTRPV5は能動的なカルシウム再吸収に重要な役割を果たしており，TRPV5ノックアウトマウスでは腎におけるカルシウム再吸収過程が破綻して，代償的に腸管からのカルシウム吸収が亢進し，$1\alpha,25(OH)_2D_3$ 産生過剰に起因する骨組織の異常が認められる[17]。

3）骨髄細胞

須田らは骨髄白血病マウスから樹立された骨髄芽球様の株細胞であるM1，あるいはヒト白血病細胞であるHL-60，U937が $1\alpha,25(OH)_2D_3$ の刺激によって単球・マクロファージ系の細胞に分化誘導され，増殖を停止させることを明らかにした[2,18]。この分化誘導作用はそれまでに知られていたリポ多糖体やデキサメタゾンなどに比較してもきわめて強力なものであり，この発見を背景としてビタミンD，あるいはビタミンD誘導体の抗腫瘍作用が注目されている。

4）皮膚

皮膚ケラチノサイトはビタミン D_3 産生に関与しているのみならず，VDR，CYP27，CYP27B1を有し，ビタミン D_3 を $25(OH)D_3$，そして $1\alpha,25(OH)_2D_3$ へと変換することができる。$1\alpha,25(OH)_2D_3$ はケラチノサイトの分化・増殖に作用するが，ケラチノサイトにおける紫外線依存性のビタミンD合成は，紫外線によるDNA障害に対する防御反応である可能性がある。すなわち $1\alpha,25(OH)_2D_3$ はケラチノサイトの $G_1 \rightarrow S$ 期への移行を抑制し，増殖を抑制することによってDNA障害抵抗性を増大させている可能性が示唆されている。$1\alpha,25(OH)_2D_3$ はケラチノサイトの分化を促進することから，尋常性乾癬のようなケラチノサイトの異常増殖を示す病態に対する治療薬として用いられている。

先にも述べたように，VDR欠損マウスあるいはビタミンD抵抗性くる病II型では脱毛が認められることから，ビタミンDと発毛との関係が注目されている。興味深いことに，このような脱毛は 1α 水酸化酵素(CYP27B1)ノックアウトマウスや 1α 水酸化酵素に異常の存在するビタミンD依存性くる病I型患者，あるいは高度のビタミンD欠乏患者では認められないこと，ケラチノサイト特異的なVDR発現によってノックアウトマウスの脱毛症が治癒することから，VDRの発毛に対する作用はリガンド非依存性であると考えられる[19]。

5）骨組織

ビタミンDが抗くる病因子として発見されたいきさつからも明らかなように，骨組織はビタミンDの主たる標的臓器である。ビタミンD欠乏状態，あるいはVDR，25位水酸化，1α 位水酸化の遺伝的障害は軟骨および骨の石灰化障害，すなわちくる病，あるいは骨軟化症を来す。またVDRノックアウトマウスは離乳直後より顕著な低カルシウム血症，二次性副甲状腺機能亢進症，進行性のくる病を示す。VDRノックアウトマウスにおいては血中の $1\alpha,25(OH)_2D$ は著しく高値を示し，逆に $24,25(OH)_2D$ 濃度はきわめて低値となる。離乳前のマウスはカルシウム代謝異常を示さないことから，この時期のマウスは $1\alpha,25(OH)_2D_3$ 非依存性のカルシウム吸収機構を有すると考えられる。しかしながら先にも述べたように，VDRノックアウトマウスを高カルシウム・高リン・高ラクトース食(レスキュー食)で飼育すると，PTH濃度や血中のイオン化カルシウム濃度は正常化し，骨組織

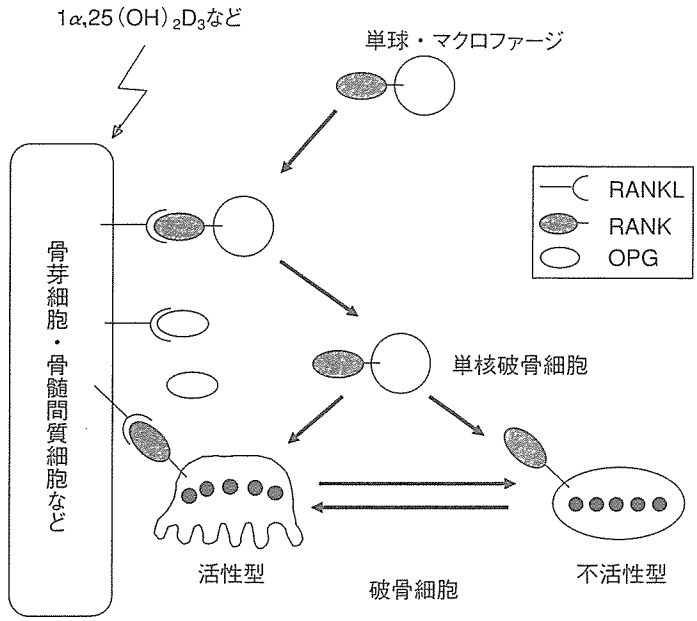

図 3　破骨細胞分化・活性化における RANKL-RANK 系の役割

の異常も治癒することが報告されている[20,21]。このような結果は，ビタミン D の骨組織に対する作用は生理的な条件においては腸管からのカルシウム吸収と腎におけるカルシウムの再吸収を介した二次的な作用が主である可能性を示唆している。しかしながら，骨組織においてさまざまな遺伝子が $1\alpha,25(OH)_2D_3$ の直接的，あるいは間接的な制御を受けていることも確かである。特に，破骨細胞分化因子である receptor activator of nuclear factor-κB ligand(RANKL)の骨芽細胞における発現が $1\alpha,25(OH)_2D_3$ によって誘導されること，そしてその生理的阻害物質であるオステオプロテジェリン(OPG)の発現が抑制されることは，骨リモデリングの調節という観点からも注目すべきであろう(図 3)。最近，骨芽細胞特異的に VDR を過剰発現したマウスにおいては皮質骨厚と骨強度の増加が認められることが報告された。この結果は，ビタミン D には骨芽細胞に対する直接的なアナボリック作用が存在する可能性を示唆するものとして注目される。

おわりに

以上，ビタミン D の代謝とその過程に関与する分子，そして活性型ビタミン D の標的細胞における役割について，最近の知見も含めて概説してきた。現在，骨粗鬆症その他のカルシウム代謝疾患に対する治療薬として，いくつかの新しいビタミン D 誘導体が開発されつつある。今後ビタミン D 代謝，作用機序のさらなる解明によって活性型ビタミン D の新たな役割が明らかになってくるかもしれない。

文　献

1) Bouillon R. Vitamin D: From photosynthesis, metabolism, and action to clinical applications. In: DeGroot LJ, Jameson JL, editors. Endocrinology. 5th ed. Philadelphia: Elsevier; 2005. p.1435-63.
2) 早川太郎，須田立雄，木崎治俊編．口腔生化学．第 3 版．医歯薬出版; 2000.

3) Rosen H, Reshef A, Maeda N, et al. Markedly reduced bile acid synthesis but maintained levels of cholesterol and vitamin D metabolites in mice with disrupted sterol 27-hydroxylase gene. J Biol Chem 1998; 273: 14805-12.
4) Cheng JB, Levine MA, Bell NH, et al. Genetic evidence that the human CYP2R1 enzyme is a key vitamin D 25-hydroxylase. Proc Natl Acad Sci USA 2004; 101: 7711-5.
5) Leheste JR, Melsen F, Wellner M, et al. Hypocalcemia and osteopathy in mice with kidney-specific megalin gene defect. FASEB J 2003; 17: 247-9.
6) Nykjaer A, Dragun D, Walther D, et al. An endocytic pathway essential for renal uptake and activation of the steroid 25-(OH)vitamin D_3. Cell 1999; 96: 507-15.
7) Tsujikawa H, Kurotaki Y, Fujimori T, et al. Klotho, a gene related to a syndrome resembling human premature aging, functions in a negative regulatory circuit of vitamin D endocrine system. Mol Endocrinol 2003; 17: 2393-403.
8) Dardenne O, Prud'homme J, Arabian A, et al. Targeted inactivation of the 25-hydroxyvitamin D_3-1α-hydroxylase gene (CYP27B1) creates an animal model of pseudovitamin D-deficiency rickets. Endocrinology 2001; 142: 3135-41.
9) Panda DK, Miao D, Tremblay ML, et al. Targeted ablation of the 25-hydroxyvitamin D 1α-hydroxylase enzyme: evidence for skeletal, reproductive, and immune dysfunction. Proc Natl Acad Sci USA 2001; 98: 7498-503.
10) St-Arnaud R, Arabian A, Travers R, et al. Deficient mineralization of intramembranous bone in vitamin D-24-hydroxylase-ablated mice is due to elevated 1,25-dihydroxyvitamin D and not to the absence of 24,25-dihydroxyvitamin D. Endocrinology 2000; 141: 2658-66.
11) Van Cromphaut SJ, Dewerchin M, Hoenderop JG, et al. Duodenal calcium absorption in vitamin D receptor-knockout mice: functional and molecular aspects. Proc Natl Acad Sci USA 2001; 98: 13324-9.
12) Yoshizawa T, Handa Y, Uematsu Y, et al. Mice lacking the vitamin D receptor exhibit impaired bone formation, uterine hypoplasia and growth retardation after weaning. Nat Genet 1997; 16: 391-6.
13) Hoenderop JG, van der Kemp AW, Hartog A, et al. Molecular identification of the apical Ca^{2+} channel in 1,25-dihydroxyvitamin D_3-responsive epithelia. J Biol Chem 1999; 274: 8375-8.
14) Peng JB, Chen XZ, Berger UV, et al. Molecular cloning and characterization of a channel-like transporter mediating intestinal calcium absorption. J Biol Chem 1999; 274: 22739-46.
15) Christakos S, Gabrielides C, Rhoten WB. Vitamin D-dependent calcium binding proteins: chemistry, distribution, functional considerations, and molecular biology. Endocr Rev 1989; 10: 3-26.
16) Freeman TC, Howard A, Bentsen BS, et al. Cellular and regional expression of transcripts of the plasma membrane calcium pump PMCA1 in rabbit intestine. Am J Physiol 1995; 269: G126-31.
17) Hoenderop JG, van Leeuwen JP, van der Eerden BC, et al. Renal Ca^{2+} wasting, hyperabsorption, and reduced bone thickness in mice lacking TRPV5. J Clin Invest 2003; 112: 1906-14.
18) Suda T, Ueno Y, Fujii K, et al. Vitamin D and bone. J Cell Biochem 2003; 88: 259-66.
19) Chen CH, Sakai Y, Demay MB. Targeting expression of the human vitamin D receptor to the keratinocytes of vitamin D receptor null mice prevents alopecia. Endocrinology 2001; 142: 5386-9.
20) Li YC, Amling M, Pirro AE, et al. Normalization of mineral ion homeostasis by dietary means prevents hyperparathyroidism, rickets, and osteomalacia, but not alopecia in vitamin D receptor-ablated mice. Endocrinology 1998; 139: 4391-6.
21) Amling M, Priemel M, Holzmann T, et al. Rescue of the skeletal phenotype of vitamin D receptor-ablated mice in the setting of normal mineral ion homeostasis: formal histomorphometric and biomechanical analyses. Endocrinology 1999; 140: 4982-7.

THE JOURNAL OF BIOLOGICAL CHEMISTRY VOL. 281, NO. 48, pp. 36846–36855, December 1, 2006

Negative Regulation of Osteoclastogenesis by Ectodomain Shedding of Receptor Activator of NF-κB Ligand*

Received for publication, July 13, 2006, and in revised form, September 6, 2006 Published, JBC Papers in Press, October 3, 2006, DOI 10.1074/jbc.M606656200

Atsuhiko Hikita[‡], Ikuo Yana[§], Hidetoshi Wakeyama[‡], Masaki Nakamura[‡], Yuho Kadono[‡], Yasushi Oshima[‡], Kozo Nakamura[‡], Motoharu Seiki[§], and Sakae Tanaka[‡1]

From the [‡]Department of Orthopaedic Surgery, Faculty of Medicine, The University of Tokyo, 7-3-1 Hongo, Bunkyo-ku, Tokyo 113-0033, and the [§]Center for Experimental Medicine, Institute of Medical Science, The University of Tokyo, 4-6-1 Shirokanedai, Minato-ku, Tokyo 108-8639, Japan

Receptor activator of NF-κB ligand (RANKL) is a transmembrane glycoprotein that has an essential role in the development of osteoclasts. The extracellular portion of RANKL is cleaved proteolytically to produce soluble RANKL, but definite RANKL sheddase(s) and the physiologic function of RANKL shedding have not yet been determined. In the present study, we found that matrix metalloproteinase (MMP) 14 and a disintegrin and metalloproteinase (ADAM) 10 have strong RANKL shedding activity. In Western blot analysis, soluble RANKL was detected as two different molecular weight products, and RNA interference of MMP14 and ADAM10 resulted in a reduction of both the lower and higher molecular weight products. Suppression of MMP14 in primary osteoblasts increased membrane-bound RANKL and promoted osteoclastogenesis in cocultures with macrophages. Soluble RANKL produced by osteoblasts from MMP14-deficient mice was markedly reduced, and their osteoclastogenic activity was promoted, consistent with the findings of increased osteoclastogenesis *in vivo*. RANKL shedding is an important process that down-regulates local osteoclastogenesis.

Receptor activator of NF-κB ligand (RANKL),[2] also known as TNF-related activation-induced cytokine, osteoprotegerin ligand, and osteoclast differentiation factor, is a type II transmembrane glycoprotein of the TNF ligand family. RANKL is expressed on the plasma membrane of osteoblasts, bone marrow stromal cells, and T-lymphocytes (1–5) and exerts its activity through binding to its TNF family receptor RANK, which is expressed on monocyte-macrophage lineage osteoclast precursors (3, 4, 6). Consequently, RANK activates downstream signaling pathways such as NF-κB, p38 mitogen-activated protein kinase, c-Jun N-terminal kinase, and nuclear factor of activated T cells c1 and leads to the differentiation, activation, and survival of osteoclasts (6–9). Both RANKL- and RANK-deficient mice develop severe osteopetrosis due to a lack of osteoclasts (10, 11). Conversely, a deficiency of osteoprotegerin (OPG), a natural inhibitor of RANKL, causes severe osteoporosis due to enhanced osteoclastogenesis (12). These findings suggest a crucial role for the RANKL/RANK/OPG axis in osteoclast development.

A number of transmembrane proteins undergo proteolysis and are released from the plasma membrane, a process called ectodomain shedding. The biologic and pathologic significance of ectodomain shedding varies between substrate proteins. For example, cytokines such as TNF-α and epidermal growth factor are released from local environments and exert their activity in paracrine and endocrine signaling by ectodomain shedding (13–15). In some cases, ectodomain shedding is necessary even for the local effects of growth factors such as epidermal growth factor (16). Although membrane-bound RANKL is converted to a soluble form through ectodomain shedding (17, 18) similar to other TNF family members, such as TNF-α (13, 14) and Fas ligand (19), the RANKL sheddases involved in physiologic and pathologic bone resorption, and the role of RANKL shedding is unknown. We report that RANKL shedding is regulated by matrix metalloproteinase (MMP) 14 and a disintegrin and metalloproteinase (ADAM) 10 in bone marrow stromal cells and osteoblasts. MMP14 is mainly involved in RANKL shedding in osteoblasts, and its deficiency up-regulates osteoclastogenesis by reducing RANKL shedding in the local bone milieu.

EXPERIMENTAL PROCEDURES

Reagents— DNA polymerase, KOD plus, was purchased from TOYOBO (Osaka, Japan). Antibodies for the His-tag were from Santa Cruz Biotechnology, Inc. (Santa Cruz, CA), antibodies for the V5 tag were from Invitrogen, antibodies for actin were from Sigma-Aldrich, and the antibody for RANKL was from Active Motif (Carlsbad, CA). MMP inhibitors, FR255031 and FR217840, were generous gifts from Astellas Pharma Inc. (Tokyo, Japan).

Constructs—The procedures for the construction of the tRANKL-SEAP expression vector, pcDNA3.1-RANKL-V5HisB, pcDNA3.1-mMMP14-V5HisA, pcDNA3.1-mMMP13-V5HisA, and expression vectors for human MT1, MT2, MT3, MT4, MT5, and MT6-MMP were described previously (20–26). An expression vector for mouse RANKL, pSG5-RANKL, was con-

* This work was supported in part by Grants-in-Aid from the Ministry of Education, Culture, Sports, Science, and Technology of Japan and the Health Science research grants from the Ministry of Health, Labor, and Welfare of Japan (to S. T.). The costs of publication of this article were defrayed in part by the payment of page charges. This article must therefore be hereby marked "*advertisement*" in accordance with 18 U.S.C. Section 1734 solely to indicate this fact.

[1] To whom correspondence should be addressed. Tel.: 81-3-3815-5415 (ext. 33376); Fax: 81-3-3818-4082; E-mail: TANAKAS-ORT@h.u-tokyo.ac.jp.

[2] The abbreviations used are: RANKL, receptor activator of NF-κB ligand; MMP, matrix metalloproteinase; ADAM, a disintegrin and metalloproteinase; OPG, osteoprotegerin; SEAP, secreted placental alkaline phosphatase; MT-MMP, membrane-type matrix metalloproteinase; siRNA, small interference RNA; PGE_2, prostaglandin E_2; IL-1, interleukin-1; M-CSF, macrophage colony-stimulating factor; ELISA, enzyme-linked immunosorbent assay; GFP, green fluorescent protein; TNF, tumor necrosis factor.

structed by inserting mouse RANKL cDNA into pSG5 (Stratagene, La Jolla, CA). Expression vectors for mouse MMP1, MMP2, MMP3, MMP7, MMP9, MMP11, MMP19, MMP23, MMP28, ADAM9, ADAM10, ADAM17, and ADAM19 were constructed by inserting the cDNA generated by reverse transcription-PCR of mRNA of mouse osteoblasts into pcDNA3.1-V5HisA (Invitrogen). The cDNA for ADAM10-V5His was further subcloned from pcDNA3.1- or ADAM10-V5HisA and inserted into the pSG5 vector. Small interference RNA (siRNA) plasmids for GFP, mouse ADAM10 and MMP14 were constructed using piGENE mU6 vector (iGENE Therapeutics Inc., Ibaraki, Japan) according to the manufacturer's protocol. Target sites were, for GFP, 5′-GCTACGTCCAGGAGCGCACCA-3′; for ADAM10, 5′-GGGTCTGTCATTGATGGAAGA-3′ and 5′-GCTGTGATTGCTCAGATATCC-3′; and for MMP14, 5′-GGACTGAGATCAAGGCCAATG-3′ and 5′- GGATGGACACAGAGAACTTCG-3′. The retrovirus vector for mouse MMP14 was constructed by inserting the cDNA fragment for mouse MMP14 into the BamHI and EcoRI restriction sites of pMX-puro (kindly provided by Toshio Kitamura, Institute of Medical Science, The University of Tokyo). Retrovirus vectors for siGFP, siMMP14, and siADAM10 were constructed as follows; cDNA fragments for siRNA, including the mouse U6 promoter were subcloned from piGENE constructs by PCR using M13F/R primers and ligated into pCR-blunt II TOPO (Invitrogen), digested by EcoRI, and inserted to the EcoRI restriction site of pMX-puro.

Cell Culture—The human kidney cell line 293T were cultured in Dulbecco's modified eagle medium (Sigma-Aldrich) and the mouse bone marrow stromal cell line TM8B2 (generous gift from Prof. Noda, Medical Research Institute, Tokyo Medical and Dental University) were cultured with α-MEM, and both of them were supplemented with 10% FBS and 1% penicillin-streptomycin solution (Sigma-Aldrich Co.). Cells were incubated at 37 °C in a humidified atmosphere containing 5% CO_2. Primary osteoblasts were harvested from the calvaria of newborn ddy (purchased from Sankyo Labo Service Co., Tokyo Japan) and C57/BL6 (MMP14-deficient mice and wild-type littermates) mice as previously described (27).

Screening of RANKL Sheddases—The alkaline phosphatase assay of the culture media and the Western blot analysis were described previously (20, 28). To detect soluble RANKL released into the culture media of TM8B2 cells, 3 ml of the culture media was incubated with 4 μl of recombinant protein G-agarose (Invitrogen) and 1 μg of recombinant OPG-Fc chimeric protein (R&D Biosystems, Minneapolis, MN) for 16 h at 4 °C, then recovered by brief centrifugation. The pellets were suspended in TNE buffer (10 mM Tris-HCl (pH 7.5), 150 mM NaCl, 1 mM EDTA, 1% Nonidet P-40), and subjected to SDS-PAGE.

Retrovirus Infection—The procedure for preparation of the retrovirus was described previously (29). Primary osteoblasts were incubated with the culture media containing retrovirus supplemented with 5 μg/ml polybrane (Sigma-Aldrich) for 16 h.

Real-time PCR—The reaction mixture for the real-time PCR was prepared using qPCR QuickGoldStar Mastermix Plus for SYBR® Green I (Nippon Gene, Tokyo, Japan), and analyzed using the ABI PRISM® 7000 Sequence Detection System (Applied Biosystems, Foster City, CA) according to the manufacturer's protocol. The set of primers used were 5′-CCCAAGGCAGCAACTTCA-3′ and 5′-CAATGGCAGCTGAGAGTGAC-3′ for mouse MMP14, 5′-TGGTGCTTCTGGACTGTCTG-3′ and 5′-TACCAGCCCAGCTTCTCAGT-3′ for mouse MT2-MMP, 5′-ATCATGGCCCCATTTTATCA-3′ and 5′-GCATTGGGTATCCATCCATC-3′ for mouse MT3-MMP, 5′-TTGAGCAGGAGGAGGAGAAA-3′ and 5′-GAGTCACCTTCTGCCACACA-3′ for mouse MT5-MMP, and 5′-AGATGTGGATCAGCAAGCAG-3′ and 5′-GCGCAAGTTAGGTTTTGTCA-3′ for mouse actin.

Western Blot of Primary Osteoblasts—Cells were treated with or without 10^{-8} M 1α,25-dihydroxyvitamin D_3 ($1\alpha,25(OH)_2D_3$), 10^{-6} M prostaglandin E_2 (PGE_2), and 10 ng/ml interleukin-1 (IL-1) for 72 h, and 10 ml of culture media were collected. Cell lysates were collected using M-PER® Mammalian Protein Extraction Reagent (Pierce) according to the manufacturer's protocol. Culture media and cell lysates were treated using the same procedure as for culture media of TM8B2.

Determination of Cleavage Sites of RANKL—pSG5-RANKL were transfected to TM8B2 cells. Seventy hours after transfection, 200 ml of the culture medium was collected, and soluble RANKL was recovered using an OPG-Fc column. Samples were subjected to SDS-PAGE, transferred to polyvinylidene membrane, and stained with Coomassie Brilliant Blue. The band was excised, and the N-terminal amino acid sequence was determined by Hokkaido System Science Co., Ltd. (Hokkaido, Japan).

ELISA—Primary osteoblasts were seeded in 48-well plates at a concentration of 1×10^5 cells/ml. If needed, cells were infected with retrovirus vectors as mentioned above. After 24 h of incubation, some cultures were treated with 10^{-8} M $1\alpha,25(OH)_2D_3$ and 10^{-6} M PGE_2 for 72 h. The concentration of RANKL in the culture media and cell lysates (homogenized in 200 μl of TNE buffer per well) was determined by ELISA system developed using a TRANCE DuoSet ELISA development kit (R&D Biosystems).

Coculture of Primary Osteoblasts and Bone Marrow Macrophages—Bone marrow macrophages were obtained from tibias of 5–8 weeks-old C57/BL6 mice by flushing the bone marrow with α-MEM, and cultured in α-MEM supplemented with 10% FBS, 1% penicillin-streptomycin solution, and 10 ng/ml M-CSF (Wako Pure Chemicals, Osaka, Japan) for 16 h, and non-adherent cells were collected. For the coculture, primary osteoblasts were seeded in 48-well plates at a concentration of 1×10^5 cells/ml. If needed, cells were infected by a retrovirus, as described above. After 24-h incubation, macrophages were seeded on the primary osteoblasts at a concentration of 1×10^5 cells/ml and treated with 10^{-8} M $1\alpha,25(OH)_2D_3$ and 10^{-6} M PGE_2 for 5 days. Osteoclasts were stained with tartrate-resistant acid phosphatase (3), and the cell number was counted. For separate culture, primary osteoblasts were cultured on the cell culture insert (BD Biosciences, San Jose, CA), and bone marrow macrophages were seeded on the bottom of 24-well plates.

Osteoclast Formation Assay by Soluble RANKL Generated by MMP14—293T cells were transfected with several combinations of pcDNA3.1-V5HisA, pcDNA3.1-RANKL-V5HisB, and pcDNA-mMMP14-V5HisA using FuGENE 6 (Roche Diagnostics, Indianapolis, IN), and 48 h after transfection, culture media were collected. Bone marrow macrophages were incubated with a 1:1 mixture of the culture media and α-MEM containing 10% FBS, supplemented with M-CSF at 10 ng/ml for 4 days.

Osteoclast Formation Assay, Survival Assay, and Pit Formation Assay of Macrophages of MMP14-deficient Mice—The MMP14-deficient mice were generated and backcrossed to the C57/BL6 strain as previously described (30). Livers and spleens were harvested from newborn MMP14-deficient mice and wild-type littermates, and cells were strained using a cell strainer. The obtained cells were incubated in α-MEM supplemented with 10% FBS, 1% penicillin-streptomycin solution, and 200 ng/ml M-CSF (Wako) for 4 days in 10-cm Petri dishes, and then M-CSF-dependent macrophages were recovered by trypsinization. For the osteoclast formation assay, macrophages were seeded in 48-well plates at a concentration of 2×10^5 cells/ml and treated with 10 ng/ml M-CSF and 100 ng/ml RANKL (Wako) for 6 days. For the survival assay and the pit formation assay, macrophages (2×10^5 cells/ml) were cocultured with primary osteoblasts (1×10^5 cells/ml) in α-MEM containing 10% FBS, 10^{-8} M $1\alpha,25(OH)_2D_3$, and 10^{-6} M PGE_2 on culture dishes precoated with 0.2% collagen gel matrix (Nitta Gelatin, Osaka, Japan). When osteoclasts were formed after 7-day culture, they were released from the dishes by treatment with 0.2% collagenase in phosphate-buffered saline, and collected by centrifugation. For the survival assay, cells were cultured on 48-well plates for 4 h, and osteoclasts were isolated by removing the osteoblasts by 0.1% collagenase and 0.2% dispase in phosphate-buffered saline. Purified osteoclasts were further incubated in α-MEM containing 10% FBS for 20 h. For the pit formation assay, cells were seeded on the dentin slices (Wako) precoated with FBS, and incubated in α-MEM containing 10% FBS, 10^{-8} M $1\alpha,25(OH)_2D_3$, and 10^{-6} M PGE_2 for 24 h. Then the cells were removed by ultrasonication after adding 1 M NH_4OH. Resorption pits were visualized by staining with 0.5% toluidine blue and analyzed using Adobe Photoshop (Adobe, San Jose, CA).

Histology—Tibias of 2- to 3-week-old male MMP14-deficient mice, and wild-type littermates were fixed in 4% paraformaldehyde and decalcified in 10% EDTA. Paraffin-embedded samples were sectioned at 5 μm and stained with hematoxylin and eosin or tartrate-resistant acid phosphatase. Observers who were blinded to the origin of the images counted the number of osteoclasts on the trabecular bone surface and measured total length of the trabecular bone using Image J software (National Institutes of Health, Bethesda, MD).

Statistical Analysis—Statistical analyses were performed using Student's *t* test for the alkaline phosphatase assay and a two-tailed unpaired Student's *t* test for the real-time PCR and ELISA. A *p* value of <0.05 was considered to be statistically significant.

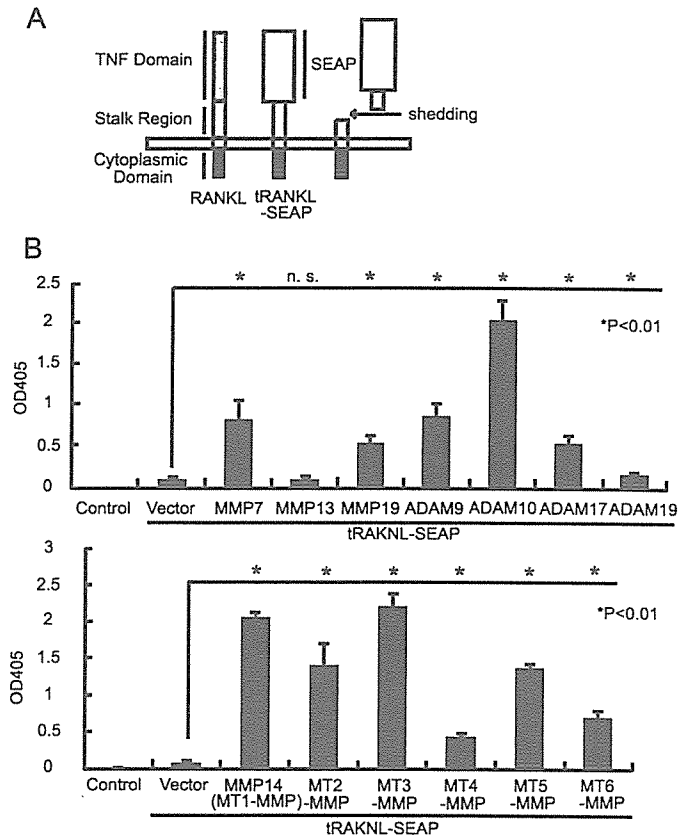

FIGURE 1. **RANKL shedding activity of MMPs and ADAMs.** *A*, schematic representation of RANKL and tRANKL-SEAP fusion protein. tRANKL-SEAP is a fusion protein of SEAP with C-terminally truncated RANKL, which contains the stalk region but lacks the TNF-like domain of RANKL, and with V5 and His× 6 tags at the C terminus. Cleavage of tRANKL-SEAP can be detected as positive alkaline phosphatase activity in the supernatants. *B*, alkaline phosphatase activity of the culture media of 293T cells transfected with pcDNA3.1-tRANKL-SEAP -V5HisA and expression vectors for ADAMs or MMPs ($n = 6$). *, significantly different, $p < 0.01$; *n. s.*, not significant.

RESULTS

Screening of MMPs and ADAMs as RANKL Sheddases—We previously developed a RANKL shedding activity screening system using an expression vector encoding a fusion protein of secreted placental alkaline phosphatase (SEAP) with the C-terminally truncated form of RANKL, which contains the stalk region, transmembrane domain, and intracellular domain of RANKL (tRANKL-SEAP) (20). Expression vectors of various MMPs or ADAMs were transfected to 293T cells together with tRANKL-SEAP plasmids, and the alkaline phosphatase activity of the culture media was measured. In this assay system, increased alkaline phosphatase activity in the medium indicates an increase in RANKL shedding (Fig. 1*A*). Several MMPs and ADAMs exhibited tRANKL-SEAP shedding activity, and ADAM10, MMP14 (membrane-type 1 matrix metalloproteinase, MT1-MMP), MT2, MT3, and MT5-MMP had relatively stronger activity (Fig. 1*B*). In contrast, MMP13 (Fig. 1*B*), MMP1, MMP2, MMP3, MMP9, MMP11, MMP23, and MMP28 (data not shown) had no tRANKL-SEAP shedding activity.

MMP14 and ADAM10 Are Major RANKL Sheddases in TM8B2 Cells—To confirm the ability of these proteinases to cleave full-length RANKL, they were overexpressed in the

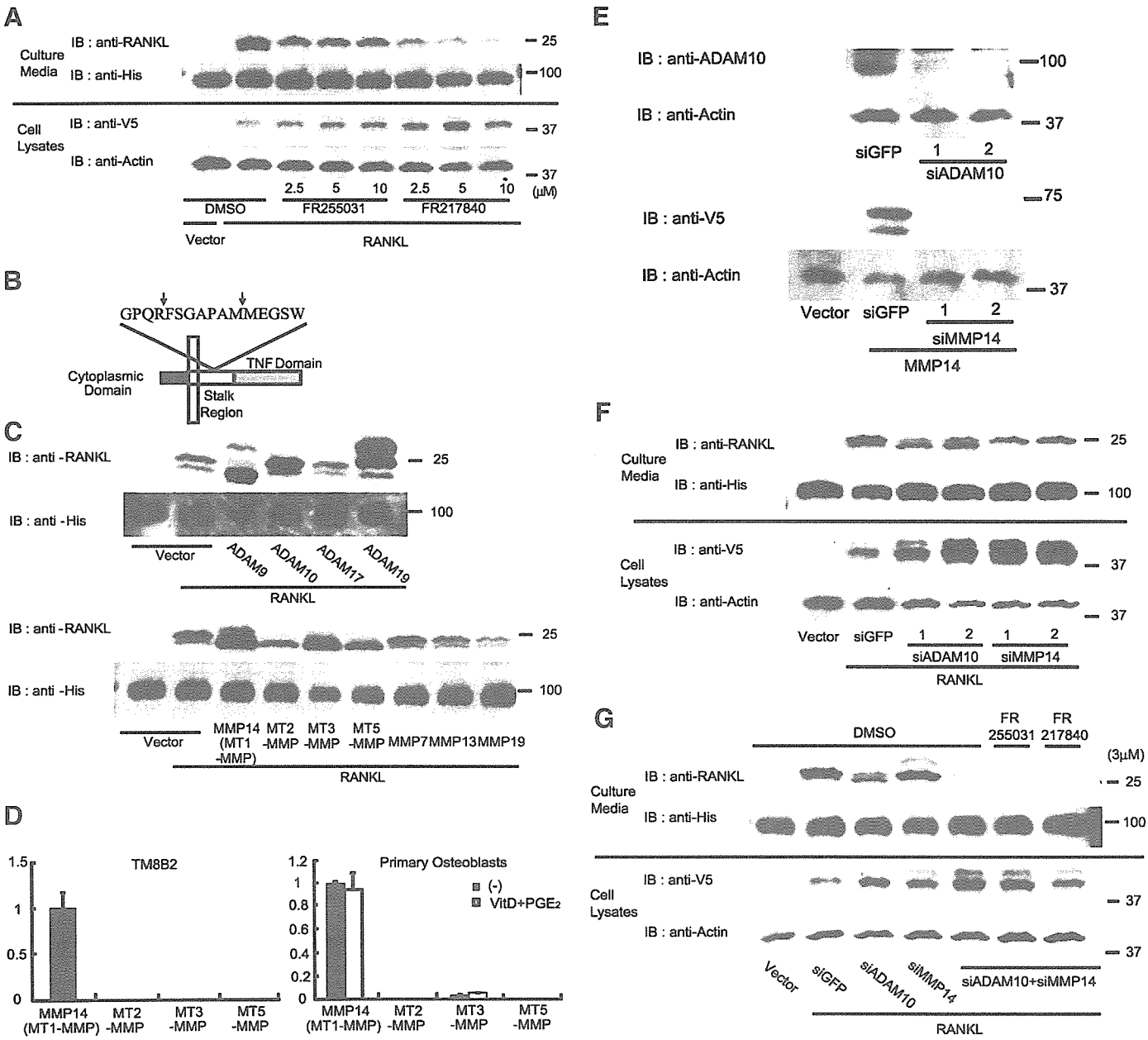

FIGURE 2. **ADAM10 and MMP14 are major RANKL sheddases in TM8B2 cells.** *A*, cleavage of full-length RANKL in TM8B2 cells transfected with pcDNA3.1-V5HisB or -RANKL. Twenty-four hours after transfection, culture media were changed to α-MEM containing either Me_2SO (*DMSO*), FR255031, or FR217840 together with 10% FBS. Culture media and cell lysates were subjected to Western blot analysis for RANKL after 72 h of incubation. Immunoblotting by anti-His shows the OPG-Fc recombinant protein used to collect soluble RANKL. *B*, schematic representation of the cleavage sites of RANKL. Cleavage sites were indicated by *arrows*. *C*, effect of ADAMs and MMPs on RANKL shedding in TM8B2 cells. TM8B2 cells were transfected with pcDNA3.1-RANKL-V5HisB and expression vectors for ADAMs or MMPs. Culture media were subjected to Western blot for RANKL 72 h after transfection. *D*, real-time PCR analysis of MT-MMP expression in TM8B2 cells and primary osteoblasts ($n = 3$). The *y*-axis represents the relative mRNA levels of the indicated genes expressed as -fold from MMP14 level. *E*, efficient gene knock-down by siADAM10 and siMMP14. TM8B2 cells were transfected with pcDNA3.1-V5HisA, piGENEmU6-siGFP, -siADAM10-1, -2, siMMP14-1, -2, or pcDNA3.1-mMMP14-V5HisA, and the expression of ADAM10 (endogenous) and MMP14 (overexpressed, detected by anti-V5 epitope tag antibody) was analyzed 48 h after transfection. *F*, Effect of siADAM10 and siMMP14 on RANKL cleavage in TM8B2 cells. TM8B2 cells were transfected with piGENEmU6-siGFP, -siADAM10-1, -2, siMMP14-1, -2, or pcDNA3.1-V5HisB, together with pcDNA3.1-RANKL-V5HisB. Seventy-two hours after transfection, culture media and cell lysates were collected and subjected to Western blot analysis. *G*, effects of siADAM10, siMMP14, and chemical inhibitors on RANKL shedding in TM8B2 cells. Procedures were the same as in *A*.

mouse bone marrow stromal cell line TM8B2 together with full-length RANKL. Soluble RANKL was recovered from the culture media using an OPG-Fc recombinant protein column and subjected to Western blot analysis. When RANKL (C-terminally tagged with V5 and 6× His) was overexpressed in TM8B2 cells (~39 kDa), there were two different molecular mass products (25 and 24 kDa) in the culture media (Fig. 2*A*). The N-terminal sequences of the two bands are shown in Fig. 2*B*. These two bands were differentially diminished by various metalloproteinase inhibitors (Fig. 2*A*). When TM8B2 cells were treated with FR255031, which inhibits several MMPs but not TNF-α secretases (31), only the lower band disappeared. On the other hand, treatment with FR217840, which not only inhibits several MMPs, but also inhibits TNF-α secretion (32), both of

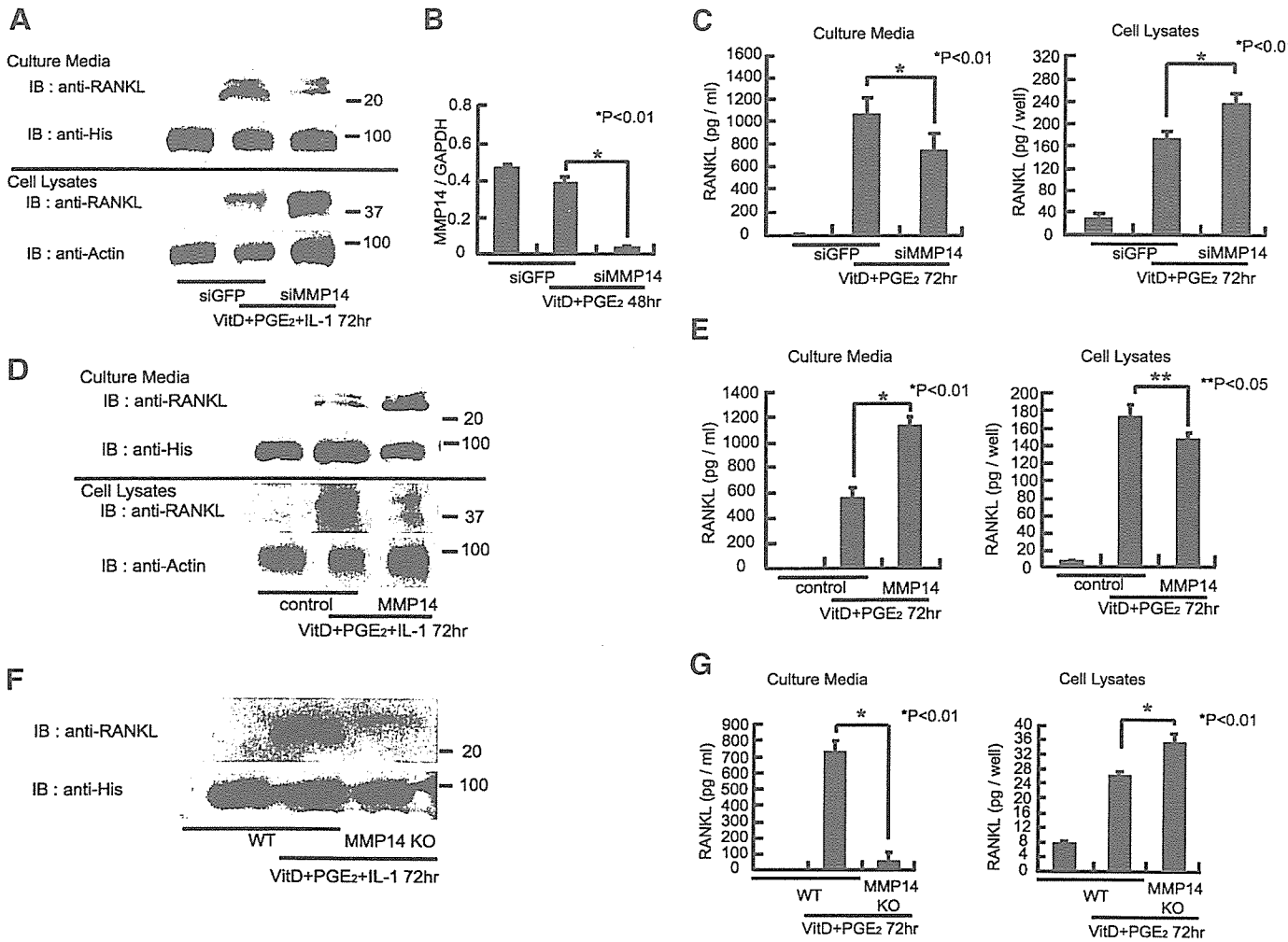

FIGURE 3. **MMP14 is a major RANKL sheddase in primary osteoblasts.** *A*, soluble and membrane-bound RANKL produced by primary osteoblasts infected with control or siMMP14 retrovirus. Twenty-four hours after infection, cells were untreated or treated with 10^{-8} M 1α,25(OH)$_2$D$_3$, 10^{-6} M PGE_2, and 10 ng/ml IL-1 for 72 h. Culture media and cell lysates were incubated with OPG-Fc fusion protein column, and the recovered proteins were subjected to Western blot analysis for RANKL. *B*, real-time PCR of MMP14 gene expression in primary osteoblasts infected with control or siMMP14 retrovirus ($n = 3$). *, significantly different, $p < 0.01$. *C*, RANKL concentration of culture media and cell lysates of primary osteoblasts as determined by ELISA ($n = 3$). Primary osteoblasts were infected with control or siMMP14 retrovirus. Twenty-four hours after infection, cells were untreated or treated with 10^{-8} M 1α,25(OH)$_2$D$_3$ and 10^{-6} M PGE_2 for 72 h. *, significantly different, $p < 0.01$. *D*, effects of retrovirus vector-mediated MMP14 overexpression on RANKL shedding in primary osteoblasts. Procedures were the same as in *A*. *E*, soluble (*left*) and membrane-bound (*right*) RANKL concentration produced by primary osteoblasts infected with control or MMP14 retrovirus ($n = 3$). Procedures were the same as in *C*. * and **, significantly different, $p < 0.01$ and $p < 0.05$, respectively. *F*, RANKL cleavage in primary osteoblasts from MMP14-deficient mice and the wild-type littermates. Cells were treated with or without 10^{-8} M 1α,25(OH)$_2$D$_3$, 10^{-6} M PGE_2, and 10 ng/ml IL-1 for 72 h. Culture media and cell lysates were incubated with osteoprotegerin-Fc fusion protein column, and the recovered proteins were subjected to Western blot analysis. *G*, RANKL concentration in culture media and cell lysates of primary osteoblasts from MMP14-deficient mouse and the wild-type littermate measured by ELISA ($n = 3$). Cells were treated with or without 10^{-8} M 1α,25(OH)$_2$D$_3$ and 10^{-6} M PGE_2 for 72 h. *, significantly different, $p < 0.01$.

the bands disappeared. These results suggest that the upper band is produced by ADAM family proteinase(s) and the lower band by MMP(s).

ADAM9, ADAM10, and ADAM19 cleaved full-length RANKL, but only ADAM10 produced soluble RANKL with the same molecular weight as the upper band observed in TM8B2 cells (Fig. 2*C*). ADAM17 did not cleave full-length RANKL. MMP14, MT2, MT3, and MT5-MMP generated soluble RANKL with the same molecular weight as the lower band. MT4- and MT6-MMP did not increase the soluble RANKL detected in the culture media (data not shown). Real-time PCR showed that the MMP14 mRNA level was much higher than that of MT2-, MT3-, or MT5-MMP in TM8B2 cells and primary osteoblasts (Fig. 2*D*), suggesting that MMP14 is mainly involved in the production of the lower band. The mRNA level of ADAM10 was comparable to that of MMP14 in these two cells (data not shown).

To determine the role of ADAM10 and MMP14 in the constitutive shedding of RANKL in TM8B2 cells, we constructed expression vectors of siRNA for ADAM10 and MMP14 (siADAM10 and siMMP14) (Fig. 2*E*). We constructed two different siADAM10 and siMMP14 vectors, and all of them effectively suppressed expression of the target molecules (Fig. 2*E*). The upper band of soluble RANKL diminished when the RANKL construct was transfected to TM8B2 cells along with siADAM10 plasmids; the lower band diminished with siMMP14 (Fig. 2*F*); and only the upper band was faintly observed when both siADAM10 and siMMP14 were transduced (Fig. 2*G*). The faint band completely disappeared in the presence of FR217840, but not FR255031 (Fig. 2*G*). These

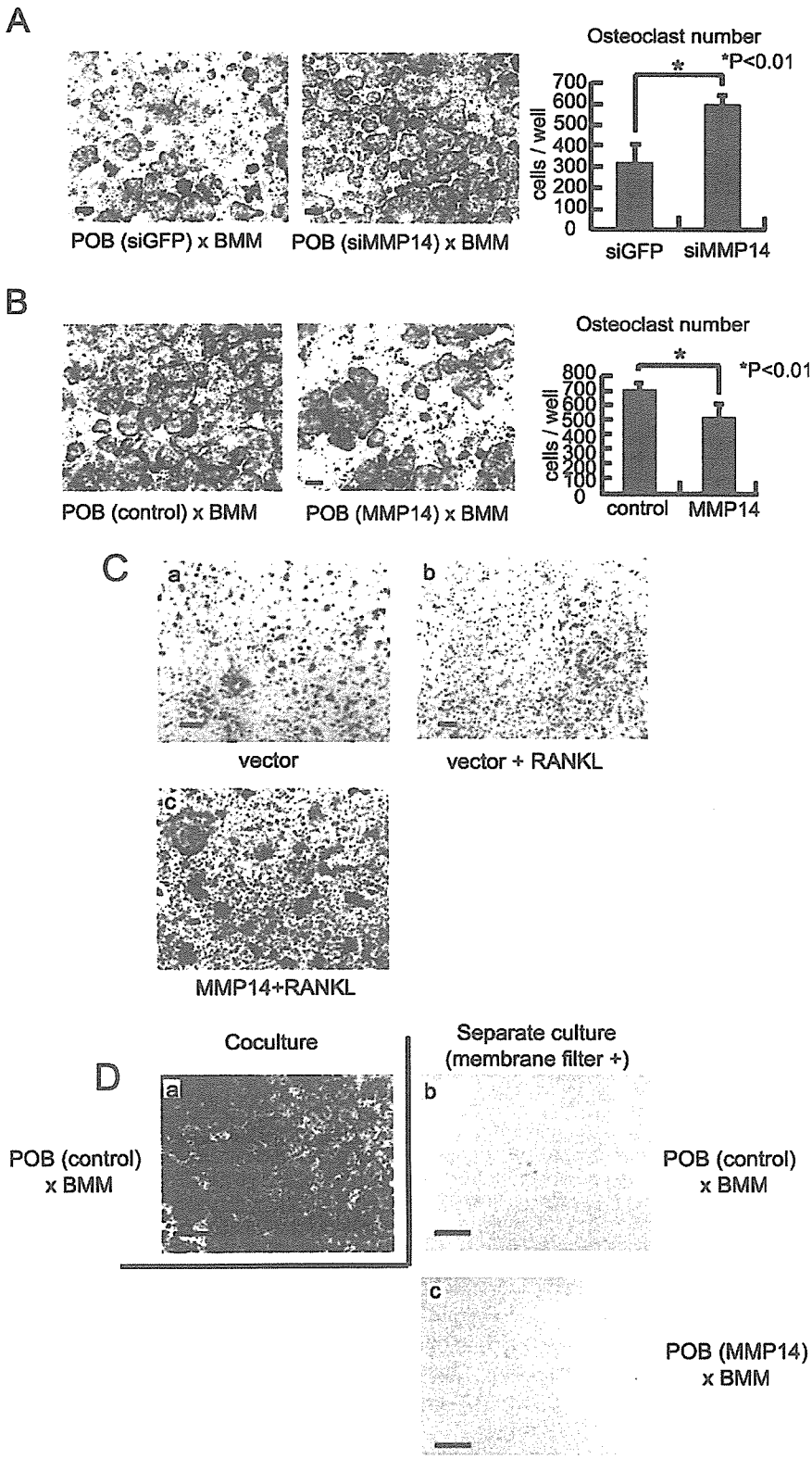

FIGURE 4. **MMP14 down-regulates osteoclastogenesis via RANKL cleavage.** *A* and *B*, coculture of primary osteoblasts infected with control siGFP or siMMP14 retrovirus (*A*), control or MMP14 retrovirus (*B*), and bone marrow macrophages. After 5 days' coculture, osteoclasts were stained with tartrate-resistant acid phosphatase and counted. *Right panel* shows the mean number of osteoclasts per well ($n = 4$). *, significantly different, $p < 0.01$. *C*, bone marrow macrophages were incubated with culture media of 293T cells transfected with pcDNA3.1-V5HisA (*a*), 1:1 mixture of pcDNA3.1-V5HisA and pcDNA3.1-RANKL-V5HisB (*b*), and 1:1 mixture of pcDNA3.1-RANKL-V5HisB and pcDNA3.1-MMP14-V5HisA (*c*), supplemented with M-CSF (10 ng/ml) for 4 days. *D*, bone marrow macrophages were cultured with primary osteoblasts infected with control (*a* and *b*) or MMP14 retrovirus (*c*) with (*b* and *c*; separate culture) or without (*a*; coculture) membrane filter between the two types of cells for 5 days. *Scale bars* = 200 μm (*A–C*) and 100 μm (*D*). *POB*, primary osteoblasts; *BMM*, bone marrow macrophages.

results indicated that ADAM10 and MMP14 are two major RANKL sheddases in TM8B2 cells.

MMP14 Cleaves RANKL in Primary Osteoblasts—We next examined the RANKL sheddases in primary osteoblasts. When primary osteoblasts were stimulated with $1\alpha,25(OH)_2D_3$, PGE_2, and IL-1, two bands appeared in the culture media with the same molecular masses (~22 and 21 kDa) as those observed in TM8B2 cells transfected with full-length RANKL without epitope tag (Fig. 3*A* and data not shown), but the lower band was more prominent. The expression of MMP14 was also much higher than that of MT2-, MT3-, or MT5-MMP in osteoblasts, suggesting that MMP14 is the major RANKL sheddase in primary osteoblasts (Fig. 2*D*). We constructed retrovirus vectors of siMMP14 that efficiently suppressed MMP14 expression in primary osteoblasts (Fig. 3*B*). When osteoblasts were infected with siMMP14 retrovirus, the lower band was diminished in the culture medium and membrane-bound RANKL was increased in the cell lysate (Fig. 3*A*). The concentration of soluble RANKL in the culture media and membrane-bound RANKL in the cell lysates was also measured by ELISA. A significant decrease in soluble RANKL and an increase in membrane-bound RANKL was observed by MMP14 knockdown (Fig. 3*C*), consistent with the results of Western blot analysis. Conversely, overexpression of MMP14 in primary osteoblasts increased the lower band of soluble RANKL in the culture media and reduced membrane-bound RANKL in the cell lysates (Fig. 3, *D* and *E*). To further confirm the role of MMP14 in RANKL shedding in osteoblasts, we analyzed primary osteoblasts obtained from MMP14 knock-out mice. When primary osteoblasts of MMP14-deficient mice were stimulated with $1\alpha,25(OH)_2D_3$, PGE_2, and IL-1, only the upper band of soluble RANKL was observed in the culture medium (Fig. 3*F*). The amount of soluble RANKL was markedly reduced in

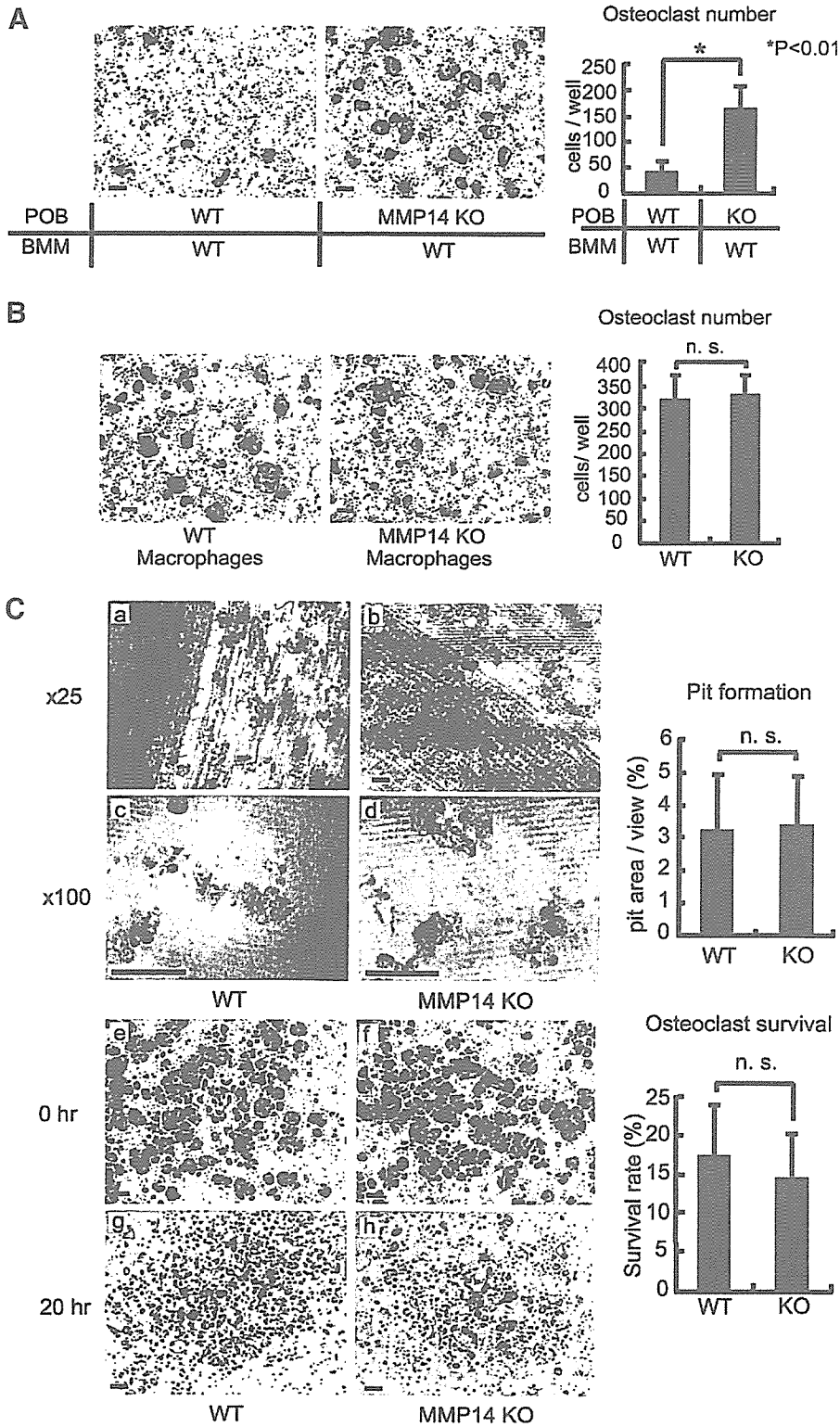

FIGURE 5. *A*, coculture of bone marrow macrophages and primary osteoblasts from MMP14-deficient mice or wild-type littermates for 5 days. *Bar* = 200 μm. *Right panel* shows the number of osteoclasts formed (n = 4). *, significantly different, $p < 0.01$. *POB*, primary osteoblasts; *BMM*, bone marrow macrophages. *B*, MMP14 deficiency does not affect osteoclast differentiation. Macrophages of MMP14 knock-out mice or wild-type littermates were cultured in the presence of M-CSF and RANKL for 6 days. *Scale bar* = 200 μm. *Right panel* shows the number of osteoclasts (n = 4). *n.s.*, not significantly different. *C*, MMP14 deficiency does not affect bone resorption activity or survival rate of osteoclasts. Macrophages of MMP14 knock-out mice (*b*, *d*, *f*, and *h*) or wild-type littermates (*a*, *c*, *e*, and *g*) were cocultured with wild-type primary osteoblasts on the collagen gel matrix for 7 days and subjected to the pit formation assay (*a–d*) and the survival assay (*e–h*). *Scale bar* = 200 μm. *Graphs* are the number of pit formation rate (*upper*), and osteoclast survival rate (*lower*) (n = 4). *n.s.*, not significantly different.

the medium, and membrane-bound RANKL was increased (Fig. 3*G*).

RANKL Shedding Negatively Regulates Osteoclastogenesis—To determine the role of MMP14 in the osteoclastogenic activity of osteoblasts, we cocultured osteoblasts infected with siMMP14 retrovirus with bone marrow macrophages. The siMMP14 retrovirus-infected osteoblasts, in which RANKL shedding activity was suppressed and membrane-bound RANKL was increased, stimulated osteoclastogenesis more effectively than control cells (Fig. 4*A*). Conversely, overexpression of MMP14 in primary osteoblasts suppressed osteoclastogenesis (Fig. 4*B*). These results suggest that membrane-bound RANKL induces osteoclastogenesis more efficiently than soluble RANKL, and the ectodomain shedding of RANKL by MMP14 negatively regulates osteoclastogenesis.

We then examined the osteoclastogenic activity of the soluble RANKL generated by MMP14. The culture media of 293T cells transfected with RANKL and MMP14 expression vectors were collected 48 h after transfection, and bone marrow macrophages were cultured in media supplemented with 10 ng/ml M-CSF (Fig. 4*C*). When macrophages were cultured in media recovered from the empty vector or RANKL expression vector-transfected cell cultures, mature osteoclasts did not form, even in the presence of M-CSF. In contrast, the culture media from the cells transfected with both RANKL and MMP14 expression vectors induced osteoclast formation, indicating that the soluble RANKL generated by MMP14 had osteoclastogenic activity. When primary osteoblasts overexpressing MMP14 by retrovirus vectors and bone marrow cells were cultured separately using cell culture inserts, which allow the passage of culture media but prevent cell-cell contact, and were stimulated with $1\alpha,25(OH)_2D_3$, PGE_2, and IL-1, very few osteoclasts were formed (Fig. 4*D*). These results suggest that the amount of endogenous

soluble RANKL generated in primary osteoblasts is not sufficient to induce osteoclastogenesis in our assay system.

We finally analyzed the osteoclastogenic activity of MMP14-deficient osteoblasts. When normal bone marrow macrophages were cocultured with osteoblasts from MMP14-deficient mice, osteoclasts were formed more efficiently than in cocultures with wild-type osteoblasts (Fig. 5*A*). On the other hand, bone marrow macrophages from MMP14-deficient mice differentiated into mature osteoclasts with the same efficiency as wild-type cells (Fig. 5*B*), and their bone-resorbing activity and survival rate were comparable (Fig. 5*C*). Consistent with these *in vitro* observations, soft x-ray images of MMP14-deficient mice displayed osteoporosis (Fig. 6*A*). Histologic sections showed thin cortical bone, decreased cancellous bone, and increased osteoclasts on the trabecular bone surface, which agreed with a previous report (33) (Fig. 6*B*). These data suggested that the increased osteoclast number in MMP14-deficient mice is due to the increase in membrane-bound RANKL in osteoblasts.

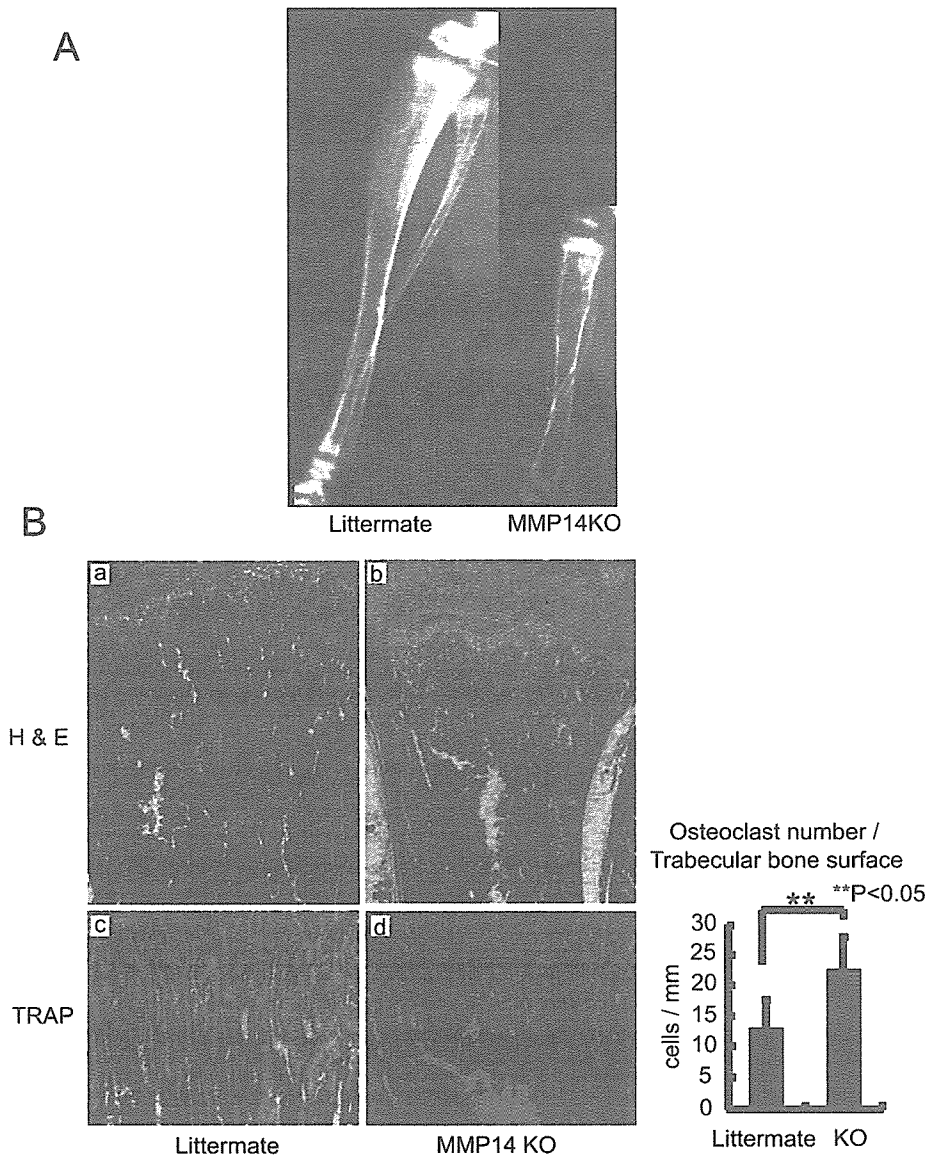

FIGURE 6. **Severe osteopenia and increased osteoclastogenesis in MMP14-deficient mice.** *A*, soft x-ray images of the left tibia of MMP14 knock-out mouse and the littermate. *B*, histologic analysis of proximal tibia of MMP14 knock-out mouse (*b* and *d*) or the wild-type littermate (*a* and *c*) stained with H&E (*a* and *b*) or tartrate-resistant acid phosphatase (*c* and *d*). *Scale bar* = 100 μm. *Right panel* shows the number of osteoclasts per trabecular bone surface ($n = 4$). **, significantly different, $p < 0.05$.

DISCUSSION

There is accumulating evidence that protein ectodomain shedding affects a large number of cellular membrane proteins, including TNF family members, but the functional outcome of shedding depends on the particular substrate protein. For example, TNF-α is cleaved by some proteinases such as TNF-α converting enzyme and released into the circulatory system to exhibit strong systemic effects (13, 14). In contrast, Fas ligand, which is a strong apoptosis inducer, has reduced effects in its soluble form (19). RANKL is a member of the TNF family of cytokines, and recent studies indicate that RANKL is essential in skeletal homeostasis for regulating the differentiation and activation of osteoclasts. Membrane-bound RANKL is proteolytically processed to generate the soluble form, but the specific proteinases involved in RANKL shedding and its physiologic and pathologic importance are not known. Western blot analysis revealed that there are two different cleaved products in the supernatants of both TM8B2 bone marrow stromal cells and primary osteoblasts, and the lower band was the major band in primary osteoblasts (Fig. 3*A*). The N-terminal sequence of the upper band coincides with the constitutive cleavage site previously reported in COS7 cells, and that of the lower band coincides with the putative MMP cleavage site. The lower band was decreased in the presence of an MMP inhibitor FR255031, and both bands were diminished by treatment with FR217840, which inhibits both MMPs and ADAMs. Previous studies also demonstrated that various MMPs and ADAMs have RANKL shedding activity (17, 20, 34–36). Therefore, we first analyzed the RANKL shedding activity of several MMPs and ADAMs using the previously reported RANKL shedding assay (20). MMP7, MMP19, ADAM9, ADAM10, ADAM17, ADAM19, MMP14, MT2, MT3, MT4, MT5, and MT6-MMP had tRANKL-SEAP shedding activity. Among these proteinases, ADAM9, ADAM10, ADAM19, MMP14, MT2, MT3, and MT5-MMP cleaved full-length RANKL. Although ADAM9 and ADAM19 had RANKL shedding activity, the molecular weights of the cleaved products were different from those con-

stitutively generated in TM8B2 cells and primary osteoblasts. Among MT-MMPs, MMP14 was predominantly expressed in TM8B2 and primary osteoblasts. MMP7 was reported to cleave RANKL *in vitro* or under overexpressing conditions and has an important role in prostate cancer-induced osteolysis (34). Although MMP7 had tRANKL-SEAP shedding activity, it did not cleave full-length RANKL in our assay system. Blobel and co-workers (17) demonstrated that ADAM17 (TNF-α converting enzyme) cleaves a partial fragment of RANKL protein, but not full-length RANKL (35), and we confirmed that ADAM17 did not cleave full-length RANKL. Although MMP13 deficiency leads to skeletal abnormalities (37), it did not cleave tRANKL-SEAP or full-length RANKL. These data, in combination with the results of siRNA experiments, led us to speculate that ADAM10 and MMP14 were major RANKL sheddases in TM8B2 cells and osteoblasts, although it is possible that other proteinases are involved in RANKL shedding in some pathologic conditions in which they are up-regulated. The functional difference between MMP14-cleaved RANKL and ADAM10-cleaved RANKL is currently under investigation.

In the culture media of primary osteoblasts, the lower molecular weight product was much more predominant than the higher molecular weight product, indicating that MMP14 is the major RANKL sheddase in primary osteoblasts. This was further confirmed by the results obtained from MMP14 knock-down osteoblasts and MMP14-deficient osteoblasts, in which the lower molecular weight band was almost completely diminished and the concentration of soluble RANKL was severely reduced.

Reduced MMP14 expression in primary osteoblasts by siRNA or its deficiency in MMP14 knock-out mouse osteoblasts reduced RANKL shedding and increased membrane-bound RANKL, which led to increased osteoclastogenic activity in the cells. Although soluble RANKL produced by MMP14 induced osteoclastogenesis from bone marrow macrophages, the culture medium of primary osteoblasts treated with $1\alpha,25(OH)_2D_3$ and PGE_2 did not induce osteoclastogenesis (38), even when MMP14 was overexpressed. This was probably due to an insufficient amount of soluble RANKL, because the concentration of the soluble RANKL in the culture media was <1 ng/ml (data not shown), and the amount of recombinant soluble RANKL necessary to induce osteoclastogenesis *in vitro* was >10 ng/ml. Still, it is possible that when the expression of RANKL is highly up-regulated, soluble RANKL has substantial effects on general bone metabolism. Gao *et al.* reported that parathyroid hormone(1–34) not only increases RANKL but also decreases MMP14 production in human osteoblasts, which might result in the efficient up-regulation of bone resorption by increasing membrane-bound RANKL in the cells (39).

In MMP14-deficient mice, generalized osteopenia was observed. Although this might be partially due to the reduced bone formation, as previously reported (33), the osteoclast number was much higher in these mice, possibly due to the increased membrane-bound RANKL in the osteoblasts. In fact, the serum level of soluble RANKL in MMP14 knock-out mice was undetectable, even when they were injected with $1\alpha,25(OH)_2D_3$ (data not shown). These phenotypes are not due to cell autonomous defects in osteoclast precursors, because there were no abnormalities in osteoclast differentiation from MMP14-deficient macrophages or bone-resorbing function of mature osteoclasts.

We were unable to determine the role of ADAM10 in *in vivo* RANKL shedding or skeletal homeostasis, because ADAM10-deficient animals die at E9.5 due to defects in heart and central nervous system development (40). Therefore, future studies using cell-specific knock-out of ADAM10 are required.

To conclude, we identified MMP14 as a major endogenous RANKL sheddase in primary osteoblasts. RANKL shedding negatively affects local osteoclastogenesis by reducing membrane-bound RANKL in the skeletal environment.

Acknowledgments—We thank R. Yamaguchi (Dept. of Orthopaedic Surgery, The University of Tokyo), who provided expert technical assistance. FR255031 and FR217840 were generously provided by Astellas Pharma Inc. (Tokyo, Japan).

REFERENCES

1. Anderson, D. M., Maraskovsky, E., Billingsley, W. L., Dougall, W. C., Tometsko, M. E., Roux, E. R., Teepe, M. C., DuBose, R. F., Cosman, D., and Galibert, L. (1997) *Nature* **390,** 175–179
2. Wong, B. R., Rho, J., Arron, J., Robinson, E., Orlinick, J., Chao, M., Kalachikov, S., Cayani, E., Bartlett, F. S., 3rd, Frankel, W. N., Lee, S. Y., and Choi, Y. (1997) *J. Biol. Chem.* **272,** 25190–25194
3. Yasuda, H., Shima, N., Nakagawa, N., Yamaguchi, K., Kinosaki, M., Mochizuki, S., Tomoyasu, A., Yano, K., Goto, M., Murakami, A., Tsuda, E., Morinaga, T., Higashio, K., Udagawa, N., Takahashi, N., and Suda, T. (1998) *Proc. Natl. Acad. Sci. U. S. A.* **95,** 3597–3602
4. Lacey, D. L., Timms, E., Tan, H. L., Kelley, M. J., Dunstan, C. R., Burgess, T., Elliott, R., Colombero, A., Elliott, G., Scully, S., Hsu, H., Sullivan, J., Hawkins, N., Davy, E., Capparelli, C., Eli, A., Qian, Y. X., Kaufman, S., Sarosi, I., Shalhoub, V., Senaldi, G., Guo, J., Delaney, J., and Boyle, W. J. (1998) *Cell* **93,** 165–176
5. Kong, Y. Y., Feige, U., Sarosi, I., Bolon, B., Tafuri, A., Morony, S., Capparelli, C., Li, J., Elliott, R., McCabe, S., Wong, T., Campagnuolo, G., Moran, E., Bogoch, E. R., Van, G., Nguyen, L. T., Ohashi, P. S., Lacey, D. L., Fish, E., Boyle, W. J., and Penninger, J. M. (1999) *Nature* **402,** 304–309
6. Tanaka, S., Nakamura, K., Takahasi, N., and Suda, T. (2005) *Immunol. Rev.* **208,** 30–49
7. Wong, B. R., Josien, R., Lee, S. Y., Vologodskaia, M., Steinman, R. M., and Choi, Y. (1998) *J. Biol. Chem.* **273,** 28355–28359
8. Takayanagi, H., Kim, S., Koga, T., Nishina, H., Isshiki, M., Yoshida, H., Saiura, A., Isobe, M., Yokochi, T., Inoue, J., Wagner, E. F., Mak, T. W., Kodama, T., and Taniguchi, T. (2002) *Dev. Cell* **3,** 889–901
9. Tanaka, S., Nakamura, I., Inoue, J., Oda, H., and Nakamura, K. (2003) *J. Bone Miner. Metab.* **21,** 123–133
10. Kong, Y. Y., Yoshida, H., Sarosi, I., Tan, H. L., Timms, E., Capparelli, C., Morony, S., Oliveira-dos-Santos, A. J., Van, G., Itie, A., Khoo, W., Wakeham, A., Dunstan, C. R., Lacey, D. L., Mak, T. W., Boyle, W. J., and Penninger, J. M. (1999) *Nature* **397,** 315–323
11. Dougall, W. C., Glaccum, M., Charrier, K., Rohrbach, K., Brasel, K., De Smedt, T., Daro, E., Smith, J., Tometsko, M. E., Maliszewski, C. R., Armstrong, A., Shen, V., Bain, S., Cosman, D., Anderson, D., Morrissey, P. J., Peschon, J. J., and Schuh, J. (1999) *Genes Dev.* **13,** 2412–2424
12. Bucay, N., Sarosi, I., Dunstan, C. R., Morony, S., Tarpley, J., Capparelli, C., Scully, S., Tan, H. L., Xu, W., Lacey, D. L., Boyle, W. J., and Simonet, W. S. (1998) *Genes Dev.* **12,** 1260–1268
13. Kriegler, M., Perez, C., DeFay, K., Albert, I., and Lu, S. D. (1988) *Cell* **53,** 45–53
14. Black, R. A., Rauch, C. T., Kozlosky, C. J., Peschon, J. J., Slack, J. L., Wolfson, M. F., Castner, B. J., Stocking, K. L., Reddy, P., Srinivasan, S., Nelson, N., Boiani, N., Schooley, K. A., Gerhart, M., Davis, R., Fitzner, J. N., Johnson, R. S., Paxton, R. J., March, C. J., and Cerretti, D. P. (1997) *Nature* **385,**

729–733
15. Harris, R. C., Chung, E., and Coffey, R. J. (2003) *Exp. Cell Res.* **284,** 2–13
16. Prenzel, N., Zwick, E., Daub, H., Leserer, M., Abraham, R., Wallasch, C., and Ullrich, A. (1999) *Nature* **402,** 884–888
17. Lum, L., Wong, B. R., Josien, R., Becherer, J. D., Erdjument-Bromage, H., Schlondorff, J., Tempst, P., Choi, Y., and Blobel, C. P. (1999) *J. Biol. Chem.* **274,** 13613–13618
18. Nakashima, T., Kobayashi, Y., Yamasaki, S., Kawakami, A., Eguchi, K., Sasaki, H., and Sakai, H. (2000) *Biochem. Biophys. Res. Commun.* **275,** 768–775
19. Schneider, P., Holler, N., Bodmer, J. L., Hahne, M., Frei, K., Fontana, A., and Tschopp, J. (1998) *J. Exp. Med.* **187,** 1205–1213
20. Hikita, A., Kadono, Y., Chikuda, H., Fukuda, A., Wakeyama, H., Yasuda, H., Nakamura, K., Oda, H., Miyazaki, T., and Tanaka, S. (2005) *J. Biol. Chem.* **280,** 41700–41706
21. Sato, H., Takino, T., Okada, Y., Cao, J., Shinagawa, A., Yamamoto, E., and Seiki, M. (1994) *Nature* **370,** 61–65
22. Takino, T., Sato, H., Shinagawa, A., and Seiki, M. (1995) *J. Biol. Chem.* **270,** 23013–23020
23. Tanaka, M., Sato, H., Takino, T., Iwata, K., Inoue, M., and Seiki, M. (1997) *FEBS Lett.* **402,** 219–222
24. Itoh, Y., Kajita, M., Kinoh, H., Mori, H., Okada, A., and Seiki, M. (1999) *J. Biol. Chem.* **274,** 34260–34266
25. Kojima, S., Itoh, Y., Matsumoto, S., Masuho, Y., and Seiki, M. (2000) *FEBS Lett.* **480,** 142–146
26. Miyamori, H., Takino, T., Kobayashi, Y., Tokai, H., Itoh, Y., Seiki, M., and Sato, H. (2001) *J. Biol. Chem.* **276,** 28204–28211
27. Suda, T., Jimi, E., Nakamura, I., and Takahashi, N. (1997) *Methods Enzymol.* **282,** 223–235
28. Yamamoto, A., Miyazaki, T., Kadono, Y., Takayanagi, H., Miura, T., Nishina, H., Katada, T., Wakabayashi, K., Oda, H., Nakamura, K., and Tanaka, S. (2002) *J. Bone Miner. Res.* **17,** 612–621
29. Kitamura, T. (1998) *Int. J. Hematol.* **67,** 351–359
30. Ohtake, Y., Tojo, H., and Seiki, M. (2006) *J. Cell Sci.* **119,** 3822–3832
31. Ishikawa, T., Nishigaki, F., Miyata, S., Hirayama, Y., Minoura, K., Imanishi, J., Neya, M., Mizutani, T., Imamura, Y., Naritomi, Y., Murai, H., Ohkubo, Y., Kagayama, A., and Mutoh, S. (2005) *Br. J. Pharmacol.* **144,** 133–143
32. Ishikawa, T., Nishigaki, F., Miyata, S., Hirayama, Y., Minoura, K., Imanishi, J., Neya, M., Mizutani, T., Imamura, Y., Ohkubo, Y., and Mutoh, S. (2005) *Eur. J. Pharmacol.* **508,** 239–247
33. Holmbeck, K., Bianco, P., Caterina, J., Yamada, S., Kromer, M., Kuznetsov, S. A., Mankani, M., Robey, P. G., Poole, A. R., Pidoux, I., Ward, J. M., and Birkedal-Hansen, H. (1999) *Cell* **99,** 81–92
34. Lynch, C. C., Hikosaka, A., Acuff, H. B., Martin, M. D., Kawai, N., Singh, R. K., Vargo-Gogola, T. C., Begtrup, J. L., Peterson, T. E., Fingleton, B., Shirai, T., Matrisian, L. M., and Futakuchi, M. (2005) *Cancer Cell* **7,** 485–496
35. Schlondorff, J., Lum, L., and Blobel, C. P. (2001) *J. Biol. Chem.* **276,** 14665–14674
36. Chesneau, V., Becherer, J. D., Zheng, Y., Erdjument-Bromage, H., Tempst, P., and Blobel, C. P. (2003) *J. Biol. Chem.* **278,** 22331–22340
37. Inada, M., Wang, Y., Byrne, M. H., Rahman, M. U., Miyaura, C., Lopez-Otin, C., and Krane, S. M. (2004) *Proc. Natl. Acad. Sci. U. S. A.* **101,** 17192–17197
38. Takahashi, N., Akatsu, T., Udagawa, N., Sasaki, T., Yamaguchi, A., Moseley, J. M., Martin, T. J., and Suda, T. (1988) *Endocrinology* **123,** 2600–2602
39. Guo, L. J., Xie, H., Zhou, H. D., Luo, X. H., Peng, Y. Q., and Liao, E. Y. (2004) *Endocr. Res.* **30,** 369–377
40. Hartmann, D., de Strooper, B., Serneels, L., Craessaerts, K., Herreman, A., Annaert, W., Umans, L., Lubke, T., Lena Illert, A., von Figura, K., and Saftig, P. (2002) *Hum. Mol. Genet.* **11,** 2615–2624

Th17 functions as an osteoclastogenic helper T cell subset that links T cell activation and bone destruction

Kojiro Sato,[1,3] Ayako Suematsu,[1,3] Kazuo Okamoto,[1,3] Akira Yamaguchi,[2] Yasuyuki Morishita,[4] Yuho Kadono,[5] Sakae Tanaka,[5] Tatsuhiko Kodama,[6] Shizuo Akira,[7] Yoichiro Iwakura,[8] Daniel J. Cua,[9] and Hiroshi Takayanagi[1,3,10]

[1]Department of Cell Signaling, [2]Department of Oral Pathology, Graduate School, and [3]COE Program for Frontier Research on Molecular Destruction and Reconstruction of Tooth and Bone, Tokyo Medical and Dental University, Tokyo 113-8549, Japan
[4]Department of Human Pathology and [5]Department of Orthopaedic Surgery, Graduate School of Medicine, University of Tokyo, Tokyo 113-0033, Japan
[6]Department of Systems Biology and Medicine, Research Center for Advanced Science and Technology, University of Tokyo, Tokyo 153-8904, Japan
[7]Department of Host Defence, Research Institute for Microbial Diseases, Osaka University, Osaka 565-0871, Japan
[8]Center for Experimental Medicine, Institute of Medical Science, University of Tokyo, Tokyo 108-8639, Japan
[9]Discovery Research, DNAX Research Inc., Palo Alto, CA 94304
[10]Solution Oriented Research for Science and Technology (SORST), Japan Science and Technology Agency (JST), Saitama 332-0012, Japan

In autoimmune arthritis, traditionally classified as a T helper (Th) type 1 disease, the activation of T cells results in bone destruction mediated by osteoclasts, but how T cells enhance osteoclastogenesis despite the anti-osteoclastogenic effect of interferon (IFN)-γ remains to be elucidated. Here, we examine the effect of various Th cell subsets on osteoclastogenesis and identify Th17, a specialized inflammatory subset, as an osteoclastogenic Th cell subset that links T cell activation and bone resorption. The interleukin (IL)-23–IL-17 axis, rather than the IL-12–IFN-γ axis, is critical not only for the onset phase, but also for the bone destruction phase of autoimmune arthritis. Thus, Th17 is a powerful therapeutic target for the bone destruction associated with T cell activation.

CORRESPONDENCE
Hiroshi Takayanagi:
taka.csi@tmd.ac.jp

Abbreviations used: BMC, BM cell; BMM, BM-derived monocyte/macrophage precursor cell; M-CSF, macrophage colony-stimulating factor; MNC, multinucleated cell; PGE_2, prostaglandin E_2; RA, rheumatoid arthritis; RANKL, receptor activator of NF-κB ligand; TRAP, tartrate-resistant acid phosphatase; T reg, regulatory T; $VitD_3$, 1,25 $(OH)_2$ vitamin D_3.

Skeletal homeostasis is dynamically influenced by the immune system (1–3), and lymphocyte- or macrophage-derived cytokines are among the most potent mediators of osteoimmunological regulation (3–7). Therefore, the effect of individual cytokines on bone cells has been extensively studied (3–7), but the subset of immune cells with selective cytokine production that specifically affects bone cell differentiation has not been well characterized. Upon activation, $CD4^+$ T cells undergo distinct developmental pathways to the specialized effector subsets: Th1 cells produce IFN-γ and regulate cellular immunity, whereas Th2 cells produce IL-4 and IL-5 and mediate humoral immunity (8). In addition, accumulating evidence suggests that newly recognized IL-17–producing T (Th17) cells have a crucial role in autoimmune inflammation (9, 10). $CD4^+CD25^+Foxp3^-$ regulatory T (T reg) cells also constitute a distinct subset that prevents immune pathology through suppression of pathogenic T cells (11). Activation of $CD4^+$ T cells is often linked to pathological bone resorption (3, 4), but the distinct $CD4^+$ T cell subset that induces the differentiation of bone-resorbing osteoclasts has not been identified (2, 3).

Osteoclasts are multinucleated cells (MNCs) of monocyte/macrophage lineage that degrade bone matrix and dynamically remodel the skeleton (4–6). The generation of osteoclasts is physiologically supported by mesenchymal cells such as osteoblasts, which provide essential signals for differentiation of the osteoclast lineage: macrophage colony-stimulating factor (M-CSF), receptor activator of NF-κB ligand (RANKL), and costimulatory signals for RANKL (12). RANKL is the key osteoclastogenic cytokine expressed by osteoclastogenesis-supporting mesenchymal cells, but the same molecule has

The online version of this article contains supplemental material.

JEM © The Rockefeller University Press $8.00
Vol. 203, No. 12, November 27, 2006 2673–2682 www.jem.org/cgi/doi/10.1084/jem.20061775

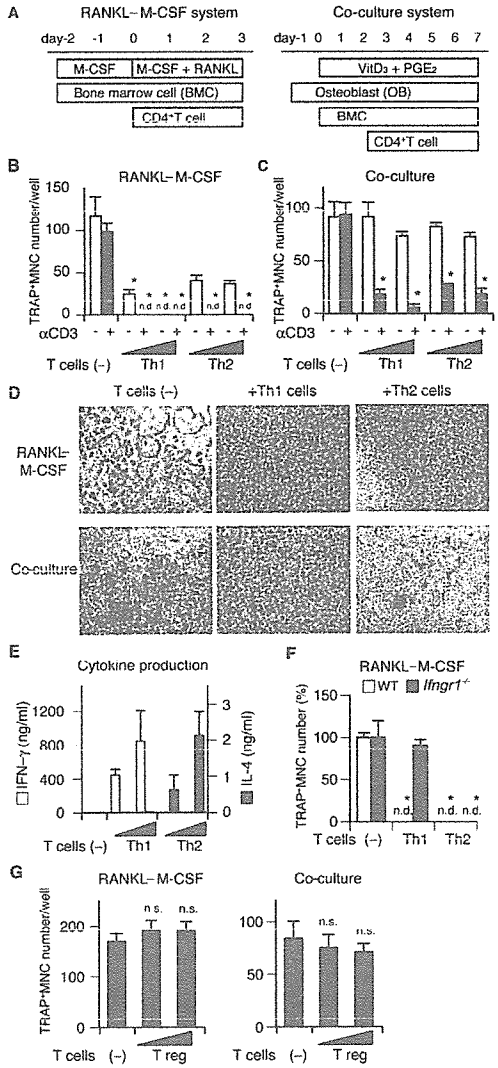

Figure 1. Effects of Th1, Th2, and T reg cells on in vitro osteoclastogenesis. (A) Schematics of two culture systems for osteoclast differentiation and Th cell addition. In the RANKL–M-CSF system, mouse nonadherent BMCs were stimulated with M-CSF for 2 d and adherent cells were used as BMMs. After BMMs were stimulated with recombinant RANKL and M-CSF for 3 d, the formation of $TRAP^+$ MNCs was analyzed. In the co-culture system, BMCs were co-cultured with osteoblasts stimulated with $VitD_3$ and PGE_2, and the formation of $TRAP^+$ MNCs was observed 7 d after the addition of BMCs. (B) Inhibitory effects of Th1 and Th2 cells on $TRAP^+$ MNC formation in the RANKL–M-CSF system. Th cells (4,000 or 20,000 cells/ml) were added at the same time as RANKL (day 0) with (black bars) or without (white bars) anti-CD3 mAb. n.d., not detected. (C) Inhibitory effects of Th1 and Th2 cells on $TRAP^+$ MNC formation in the co-culture system. The same number of T cells as in B was added 2 d after BMC addition (day 2). (D) Microphotographs of the in vitro osteoclast formation systems in the presence of Th1 or Th2 cells (20,000 cells/ml) with anti-CD3 mAb ($TRAP^+$ staining). (E) Cytokine profile of culture supernatants in the presence of Th cells and 1 μg/ml of soluble anti-CD3 mAb (the RANKL–M-CSF system on day 2). Without restimulation by anti-CD3 mAb, cytokine production was much less than this result and was difficult to detect after 2-d culture with osteoclast precursor cells (not depicted). (F) Effects of Th1 and Th2 cells (20,000 cells/ml plus anti-CD3 mAb) on WT or IFN-γ receptor–deficient (*Ifngr1*$^{-/-}$) osteoclast precursor cells. (G) Effects of isolated $CD4^+CD25^+$ T reg cells (4,000 or 20,000 cells/ml plus anti-CD3 mAb) on osteoclastogenesis in vitro. n.s., not significantly different. The survival of a considerable number of T reg cells after 3 d was confirmed by CFSE staining (not depicted).

been shown to be expressed by T cells, indicating that RANKL is a molecule that bridges the skeletal and immune systems (4).

In autoimmune arthritis, bone destruction is attributable to excessive bone resorption by osteoclasts, the formation of which is directly and indirectly regulated by $CD4^+$ T cells infiltrating into the lesion (2, 3, 13, 14). Indirect effects are mainly mediated by inflammatory cytokines produced by macrophage-like synovial cells such as TNF-α and IL-1 that induce RANKL on synovial fibroblasts (14–16), but it is poorly understood how T cells exert direct effects (3). Although T cells express RANKL, the T cell–mediated positive effect is not easily observed because T cells also produce IFN-γ, which counterbalances the effect of the RANKL, making the net effect on osteoclastogenesis inhibitory (3, 13, 14). Although autoimmune arthritis has traditionally been assumed to be a Th1 disease (17, 18), there is controversy over the role of Th1 cells in the onset phase of the disease based on the observations that typical Th1 cytokines, such as IFN-γ, are not always highly expressed in the lesion (19, 20), and that collagen-induced arthritis is exacerbated in mice lacking IFN-γ signaling (21, 22). Therefore, neither bone destruction nor inflammation may be attributable to Th1 cells. It is a critically important issue to determine the type of T cells linked to the activated osteoclastogenesis under such inflammatory conditions.

Recently, it has been reported that the IL-23–IL-17 axis, rather than the IL-12–IFN-γ axis, is critical for the onset of autoimmune arthritis (23, 24). It is also reported that IL-17 is detectable in the synovial fluid from rheumatoid arthritis (RA) patients and enhances osteoclastogenesis by inducing RANKL on mesenchymal cells (25). Here, we explored the effects of various $CD4^+$ T cell subsets on osteoclast differentiation and identified Th17 cells as the exclusive osteoclastogenic T cell subset among the known $CD4^+$ T cell lineages. The importance of the IL-23–IL-17 axis in the bone destruction phase was underscored by the observations in mice lacking either IL-17 or IL-23 (p19). We also found that the mRNA expression of *RANKL* correlates with that of *IL-23* (*IL23A*), but not that of *IL-12* (*IL12A*), in the synovial tissues of RA patients. Collectively, these results suggest that autoimmune arthritis can be deemed a Th17-type disease in terms of both the onset and destruction phases and provide a molecular basis for targeting the IL-23–IL-17 axis in the treatment of RA.

RESULTS

Effects of Th1, Th2, and T reg cells on osteoclastogenesis

Although the effects of activated T cells on osteoclastogenesis have been documented in previous reports (13, 14, 26), these

T cells were only stimulated by anti-CD3 antibody or PMA and the characterization of the T cells was not strictly performed. In this study, to investigate the effects of effector Th cell subsets on osteoclastogenesis, we added Th subsets, which were strictly developed under Th1 or Th2 conditions. Purified $CD4^+$ T cells were stimulated with anti-CD3/CD28 mAbs in the presence of either IL-12 (with anti–IL-4 mAb) or IL-4 (with anti–IFN-γ mAb) for Th1 or Th2 polarization. The Th cells were added to the two types of in vitro osteoclast differentiation systems: osteoclast precursor cells derived from BM cells (BMCs) were stimulated with recombinant RANKL and M-CSF (the RANKL–M-CSF system), or co-cultured with osteoblasts in the presence of 1,25 $(OH)_2$ vitamin D_3 ($VitD_3$) and prostaglandin E_2 (PGE_2) (the co-culture system), and the formation of MNCs stained for tartrate-resistant acid phosphatase (TRAP), a marker enzyme for osteoclasts, was evaluated (Fig. 1 A). When Th1 or Th2 cells were added to the RANKL–M-CSF system at the same time as RANKL, both subsets had a marked inhibitory effect on the formation of $TRAP^+$ MNCs and the inhibitory effects were dependent on the number of added T cells (Fig. 1, B and D). These inhibitory effects were significantly enhanced by re-stimulation with soluble anti-CD3 mAb, suggesting that re-stimulation of T cell receptor augments the polarized cytokine secretion and the inhibitory effects on osteoclastogenesis. If Th1 or Th2 cells were added to the co-culture system 2 d after BMC addition, the inhibitory effects of both subsets on osteoclastogenesis were exerted only by T cells restimulated with anti-CD3 mAb (Fig. 1, C and D). Th1 and Th2 cells both had less suppressive effects in the co-culture system, possibly because osteoblasts provide protection against the inhibitory effects through costimulatory signals (27) (see Discussion). As expected, the Th1 and Th2 subsets used in these experiments produced a significant amount of IFN-γ and IL-4, respectively (Fig. 1 E). The inhibitory effects of Th1 cells on osteoclastogenesis were completely abrogated on the BM-derived monocyte/macrophage precursor cells (BMMs) derived from IFN-γ receptor–deficient (*Ifngr1*$^{-/-}$) mice (28), indicating that IFN-γ is responsible for the Th1 cell–mediated inhibition of osteoclastogenesis (Fig. 1 F). We further analyzed the effects of $CD4^+CD25^-$ T reg cells on osteoclastogenesis in both systems, but they were found to have neither an enhancing nor an inhibitory effect (Fig. 1 G), suggesting that T reg cells are not directly related to the T cell–mediated regulation of bone resorption.

Characterization of MNCs induced by Th2 cells and IL-4

It has been reported that the inhibitory effect of IFN-γ on osteoclastogenesis is reduced if the osteoclast precursor cells encounter RANKL before IFN-γ stimulation, suggesting that RANKL-prestimulated preosteoclasts are resistant to such inhibitory cytokines (29). To test whether the inhibitory effects of Th cells on osteoclastogenesis are also dependent on the differentiation stage of the osteoclast precursor cells, we added the Th cells to the osteoclast formation systems 1 d later than in the previous experiment. Interestingly, the inhibitory effects of Th cells were less (Fig. 2 A). Although Th1 cells inhibited the formation of $TRAP^+$ MNCs under this condition, Th2 cells induced a normal number of $TRAP^+$ MNCs in the RANKL–M-CSF system and even an increased number in the co-culture system (Fig. 2 A).

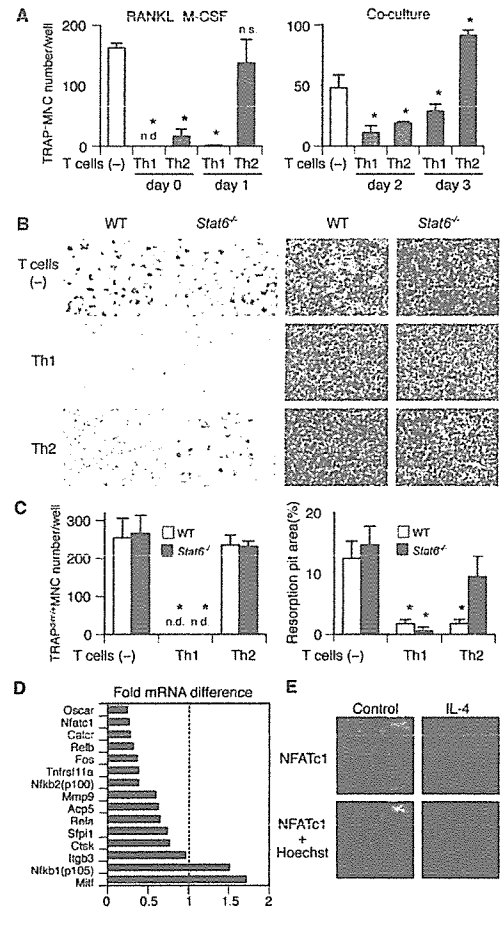

Figure 2. Formation of multinuclear cells with no bone-resorbing activity induced by Th2 cells and IL-4. (A) Inhibitory effects of Th1 and Th2 cells on osteoclastogenesis are reduced when T cells are added 1 d later. Th cells (20,000 cells/ml plus anti-CD3 mAb) were added on days 0 (at the same time as RANKL, gray bars) or 1 (black bars) to the RANKL–M-CSF system and on days 2 (2 d after BMC addition, gray bars) or 3 (black bars) to the co-culture system. (B) Microphotographs and (C) quantification of in vitro osteoclast formation (left, TRAP staining) and resorption pit formation (right). Th1 and Th2 cells (20,000 cells/ml plus anti-CD3 mAb) were added to WT or *Stat6*$^{-/-}$ osteoclast precursor cells on day 1. (D) Effect of IL-4 on mRNA expression of osteoclast-related genes in osteoclast precursor cells (GeneChip analysis). Osteoclast precursor cells were stimulated by 10 ng/ml IL-4 from day 1 in the RANKL–M-CSF system and harvested on day 3. Fold mRNA difference was calculated by dividing the average difference of the IL-4–treated sample by that of the control sample. The expressions of most of the osteoclast-specific genes are down-regulated. (E) Reduced expression of NFATc1 protein in the cells treated with IL-4. Osteoclast precursor cells were stimulated by 10 ng/ml IL-4 from day 1 in the RANKL–M-CSF system, fixed on day 3, and stained with anti-NFATc1 antibody followed by Alexa Fluoro 488–labeled secondary antibody

These results appeared to suggest that Th2 cells increase osteoclastogenesis under certain conditions, but the MNCs induced in the presence of Th2 cells were only weakly stained for TRAP ($TRAP^{dim}$) and were incapable of bone resorption (Fig. 2, B and C). Even in the presence of Th2 cells, $TRAP^{+}$ MNCs with bone-resorbing activity were formed from BMMs derived from mice deficient in Stat6, which is an essential mediator of IL-4 signaling (30), suggesting that IL-4 is involved in the formation of $TRAP^{dim}$ MNCs. Consistent with this, the addition of IL-4 to the RANKL–M-CSF system at the same time as RANKL strongly inhibited $TRAP^{+}$ MNC formation, and the addition of IL-4 1 d later induced $TRAP^{dim}$ MNCs (Fig. S1, available at http://www.jem.org/cgi/content/full/jem.20061775/DC1). The effects of IL-4 were abrogated if added to Stat6-deficient cells, which generated $TRAP^{+}$ MNCs that were able to resorb bone.

To further characterize the $TRAP^{dim}$ MNCs induced by Th2 cells through IL-4, we performed a genome-wide microarray screening of the genes expressed in the $TRAP^{dim}$ MNCs (31). $TRAP^{dim}$ MNCs induced by IL-4 expressed a high level of genes characteristic of activated macrophages, including chemokine ligands and enzymes involved in allergic responses (Fig. S2, available at http://www.jem.org/cgi/content/full/jem.20061775/DC1). The expression of most of the genes important for osteoclast differentiation or functions was decreased (Fig. 2 D). The expression of NFATc1, an essential transcription factor for osteoclastogenesis (31, 32), was also revealed to be down-regulated by immunostaining (Fig. 2 E). Thus, the $TRAP^{dim}$ MNCs induced by Th2 cells are not authentic osteoclasts but rather should be classified as macrophage polykarions.

Th17 cells stimulate osteoclastogenesis through osteoclastogenesis-supporting cells

Because the above results show that neither Th1, Th2, nor T reg cells enhance osteoclastogenesis, we next focused on a newly identified $CD4^{+}$ T cell subset producing IL-17 called Th17 (33, 34). We suspected the Th17 subset to be a good candidate for the osteoclastogenic Th subset because it has been reported that IL-17 induces RANKL on mesenchymal cells and promotes osteoclastogenesis in vitro (25). Moreover, Th17 cells, which produce IL-17 (IL-17A) and its related cytokines such as IL-17F, but not IFN-γ or IL-4, are responsible for a variety of autoimmune inflammatory effects (9, 10). Recent studies suggest that TGF-β and IL-6 are essential for the initiation of Th17 differentiation and IL-23 is critical for expanding the population (35, 36). IL-23 is one of the IL-12 family cytokines and is a heterodimer consisting of the subunits p40 and p19 (9, 10). Even though IL-23 shares a p40 subunit and one of its receptor subunits (IL-12β1) with

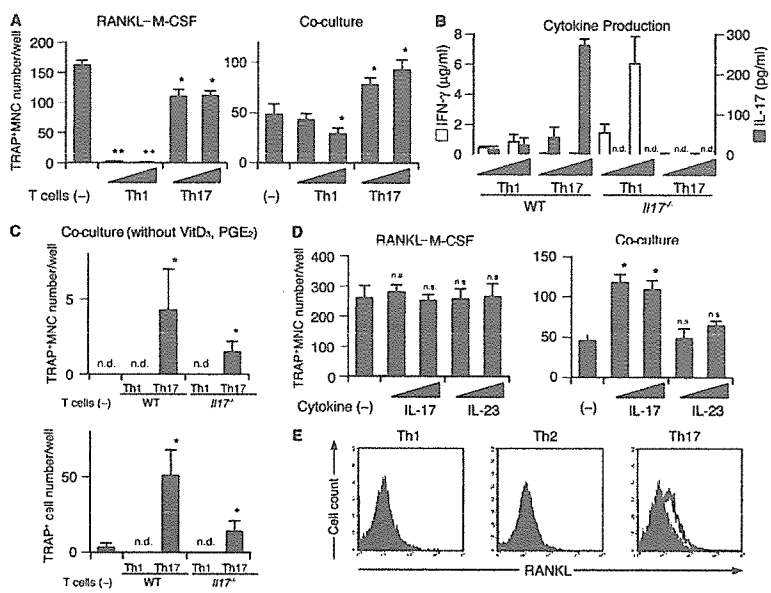

Figure 3. Enhanced osteoclastogenesis by Th17 cells in the co-culture system but not in the RANKL–M-CSF system. (A) Effects of Th1 and Th17 cells on the osteoclast differentiation systems. T cells (4,000 or 20,000 cells/ml plus anti-CD3 mAb) were added on day 1 to the RANKL–M-CSF system and on day 3 to the co-culture system. When the Th17 cells were added 1 d earlier, or in the absence of soluble anti-CD3 mAb, enhancement of osteoclastogenesis was not observed even in the co-culture system (not depicted). (B) Cytokine profile of the culture supernatants obtained on day 3 from the RANKL–M-CSF system in the presence of Th1 and Th17 cells derived from either WT or *Il17*$^{-/-}$ mice under the conditions described in A. (C) Effects of Th1 and Th17 cells derived from either WT or *Il17*$^{-/-}$ mice on the formation of $TRAP^{+}$ MNCs or $TRAP^{+}$ cells in the co-culture system in the absence of $VitD_3$ and PGE_2. T cells (20,000 cells/ml plus anti-CD3 mAb) were added on day 3. (D) Effects of recombinant IL-17 and IL-23 (2 or 10 ng/ml) on osteoclastogenesis in vitro. (E) Expression of RANKL on Th subsets. $CD4^{+}$ T cells cultured in each of the Th conditions for 3 d were restimulated with 1 μg/ml of plate-bound anti-CD3 mAb for 4 h and subjected to flow cytometric analysis using anti-RANKL mAb. Without the restimulation by anti-CD3 mAb, RANKL expression was barely detectable (not depicted).

IL-12, IL-23 and IL-12 selectively play critical roles in the regulation of Th1 and Th17 polarization, respectively.

To obtain the Th17 cells, we stimulated $CD4^+$ T cells with anti-CD3/CD28 mAbs in the presence of IL-23, anti–IFN-γ mAb, and anti–IL-4 mAb. In the presence of Th17 cells, $TRAP^+$ MNCs were efficiently formed in the RANKL–M-CSF system (Fig. 3 A) and possessed bone-resorbing activity (not depicted), although the efficiency is a little less than in the control culture without the T cells. Moreover, in the co-culture system, the Th17 cells significantly enhanced the formation of $TRAP^+$ MNCs (Fig. 3 A). Consistent with the previous reports, Th17 cells used in the above experiments produced a large amount of IL-17 but little IFN-γ, but Th1 cells did the opposite (Fig. 3 B). When Th17 cells were added to the co-culture system even in the absence of $VitD_3$ and PGE_2, the formation of $TRAP^+$ MNCs was observed (Fig. 3 C). The osteoclastogenic effects of Th17 cells in the co-culture system was greatly reduced when we used Th17 cells derived from *Il17*$^{-/-}$ mice (37), indicating that the IL-17 produced from Th17 cells is mainly responsible for the osteoclastogenic effects of Th17 cells. IL-23 or IL-17 had no effect on osteoclastogenesis in the RANKL–M-CSF system, but IL-17 promoted osteoclastogenesis in the co-culture system, suggesting that IL-17 does not directly act on osteoclast precursor cells but rather on osteoclastogenesis-supporting cells (Fig. 3 D). This is consistent with the previous report that IL-17 promotes osteoclastogenesis through the induction of RANKL on osteoblastic cells (25). These results show that Th17 is the only osteoclastogenic Th subset according to the currently accepted categorization of $CD4^+$ T cells, and that Th17 cells facilitate osteoclastogenesis, possibly through IL-17–mediated induction of RANKL on osteoblastic cells.

We evaluated the expression level of RANKL on the surface of Th cells and found that Th17 cells express a significant amount of RANKL, but Th1 cells express only a minimal amount (Fig. 3 E). Neither subset, however, exhibited promotive effects on osteoclastogenesis in the RANKL–M-CSF system (Fig. 3 A) or induced any $TRAP^+$ cells when added to the BMM culture in the absence of exogenous soluble RANKL (not depicted). Thus, it is evident that the RANKL expressed by Th cells alone is not sufficient to activate osteoclastogenesis (see Discussion).

The IL-23–IL-17 axis plays a critical role in inflammation-induced bone destruction in vivo

To clarify the role IL-17 and IL-23 play in bone metabolism in vivo, we investigated the phenotype of *Il17*$^{-/-}$ and *Il23a*$^{-/-}$ (lacking p19) (38) mice. There was no significant difference in bone mineral density as evaluated by dual-energy x-ray absorptiometry (Fig. 4 A). Microradiography also

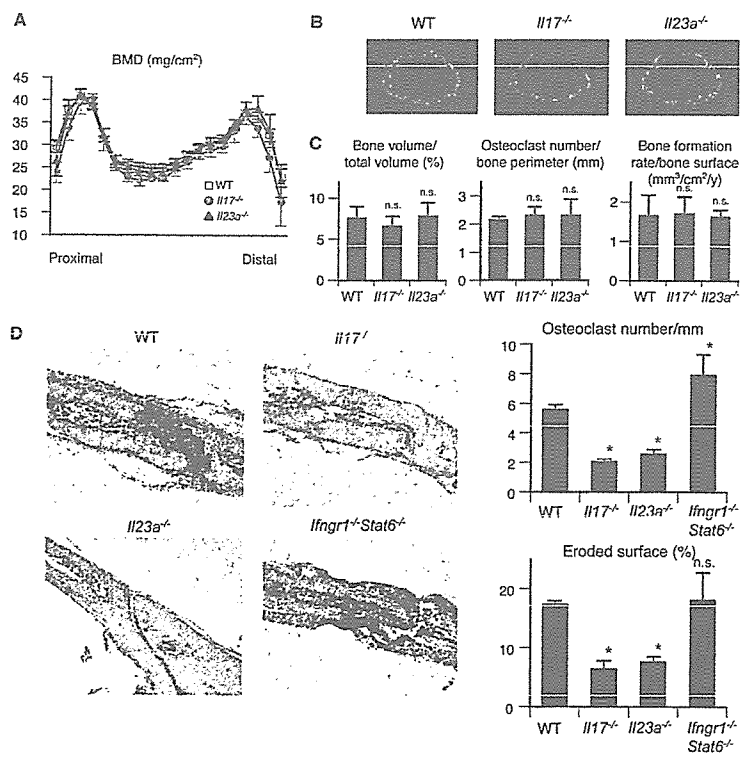

Figure 4. Contribution of IL-17 and IL-23 to the physiological and pathological bone resorption. (A) Bone mineral densities (measured in 20 longitudinal divisions of the femurs), (B) micro-computed tomography (at 10% length above the distal epiphyseal plate), and (C) bone morphometric analyses of WT, *Il17*$^{-/-}$, and *Il23a*$^{-/-}$ mice at the age of 12 wk. (D) Histological examination of calvarial bones of WT, *Il17*$^{-/-}$, and *Il23a*$^{-/-}$ mice treated with LPS (hematoxylin and TRAP staining). The degree of bone destruction was analyzed by the number of osteoclasts and the area of the eroded surface (%).

revealed no obvious abnormality in skeletal development (Fig. 4 B). Bone morphometric analyses revealed the parameters of bone resorption and formation to be normal even in the mutant mice (Fig. 4 C), indicating that neither IL-17 nor IL-23 is involved in the physiological regulation of bone homeostasis.

To further investigate the role of IL-17 and IL-23 in the disease conditions characterized by enhanced osteoclastogenesis associated with T cell activation, we used an LPS-induced model of inflammatory bone destruction, which is not induced by an autoantigen but is T cell dependent (14, 39). Because it is well documented that IL-17 and IL-23 play an important role in the development of autoimmune arthritis (23, 24), we used this inflammatory bone destruction model to evaluate their role in the osteoclast-mediated destruction phase. LPS injection into the calvarial bone results in severe bone destruction associated with aberrant formation of osteoclasts in WT mice, but the level of bone destruction was much less pronounced and the osteoclast formation was significantly reduced in both the *Il17*$^{-/-}$ mice and *Il23a*$^{-/-}$ mice (Fig. 4 D). These results suggest that the Th17 cells expanded through IL-23 stimulation are involved in the T cell–mediated osteoclastogenesis in vivo. In contrast, the bone destruction was enhanced and a greater number of osteoclasts were formed in *Ifngr1*$^{-/-}$ *Stat6*$^{-/-}$ mice, which are deficient in the response to both IFN-γ and IL-4 (Fig. 4 D), suggesting that IFN-γ and IL-4 may play a protective role against bone destruction by suppressing osteoclastogenesis associated with inflammation.

The above results suggest that IL-23–stimulated proliferation of Th17 cells, a major osteoclastogenic Th subset, plays a pivotal role in inflammatory bone destruction by inducing RANKL through an IL-17 effect on mesenchymal cells. Consistent with this, it has been reported that RANKL is abundantly expressed in the synovial fibroblasts of RA patients (16, 40) and the IL-17 concentration is elevated in the synovial fluid of RA patients (25). To explore the role of IL-23 in the induction of RANKL in RA, we investigated whether IL-23 was detected in the synovium of RA patients. Quantitative RT-PCR analysis revealed the mRNA of the p19 subunit of IL-23 (*IL23A*) in all the samples of the synovium derived from RA patients, and the expression level of *IL23A* positively correlated with that of *RANKL* (Fig. 5 A). A similar correlation was observed between *RANKL* and the p40 subunit shared by IL-12 and IL-23 (*IL12B*), but the expression of the p35 subunit specific for IL-12 (*IL12A*) did not correlate with that of *RANKL*, suggesting that IL 23 is an important determinant of arthritic bone destruction through the induction of RANKL. These results lend further support to the notion that the IL-23–IL-17 axis, rather than the IL-12–IFN-γ axis, is critical for the bone destruction phase of autoimmune arthritis.

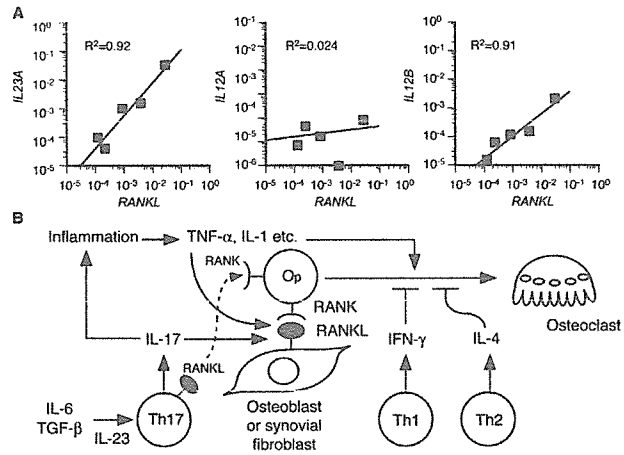

Figure 5. Regulation of RANKL-mediated osteoclastogenesis by the IL-23–IL-17 axis in the RA synovial tissue. (A) Correlation of the mRNA expression level of RANKL with that of *IL23A* (*p19*), *IL12A* (*p35*), or *IL12B* (*p40*) in the synovium of RA patients. The relative expressions of *RANKL*, *IL23A*, *IL12A*, and *IL12B* were all standardized using that of *GAPDH*. (B) Model of Th17-mediated bone destruction in autoimmune arthritis. Th17 cells function as an osteoclastogenic Th cell subset by stimulating local inflammation, inducing RANKL on osteoclastogenesis-supporting cells, and expressing RANKL on themselves, all of which contribute to an acceleration of osteoclastogenesis. It is notable that RANKL on Th17 cells alone is not sufficient for the induction of osteoclast differentiation (a dotted line). See Discussion for the details. Op, osteoclast precursor cell.

DISCUSSION

Coordinated activation of the innate and adaptive immune systems is essential for the efficient eradication of pathogens, but aberrant or prolonged activation under certain pathological conditions, such as autoimmune inflammation, results in tissue damage through the activation of effector cells. In autoimmune arthritis, it has long been a challenging question as to how the abnormality of the immune system induces the skeletal damage, although the infiltration of $CD4^+$ T cells in the RA synovium is a pathogenetic hallmark and is undoubtedly linked to the bone destruction that ensues (3, 13, 14, 20). After RANKL was cloned and the high RANKL expression in the synovium was brought to light (16, 40), the importance of bone-resorbing osteoclasts came into general acceptance (3). Based on recent reports using genetically modified mice, the crucial role of osteoclasts in the inflammatory bone loss has been established (41, 42), but which $CD4^+$ T cells cause the induction of osteoclasts, and by what mechanism, has remained elusive.

As RANKL is expressed in activated T cells, T cells may have the capacity to induce osteoclast differentiation by directly acting on osteoclast precursor cells (13, 26). However, because T cells also secrete a variety of cytokines and express membrane-bound factors other than RANKL, the effects of T cells on osteoclastogenesis should be dependent on the balance of positive and negative factors expressed by the T cells. As summarized in Fig. 5 B, the results in this study show that Th1 and Th2 cells inhibit osteoclastogenesis by acting on the precursor cells, mainly through IFN-γ and IL-4, respectively.

The inhibitory effects of these cytokines were less observed in the co-culture system than in the RANKL–M-CSF system (Figs. 1, B and C, and 2 A). We infer that osteoblasts may provide membrane-bound RANKL and stimulate costimulatory signals for RANKT simultaneously, enabling the strong cell–cell contact between osteoblasts and osteoclast precursor cells and preventing the access of T cells or inhibitory cytokines to osteoclast precursor cells.

Previous observations that IL-12 and IL-18, which drive Th1 differentiation, both inhibit osteoclastogenesis via IFN-γ or GM-CSF (43, 44), and that IL-10, which is released from Th2 cells, also negatively regulates osteoclastogenesis (45) further support the negative role of Th1 and Th2 cells on osteoclastogenesis. In contrast, Th17 cells stimulated by IL-23 promote osteoclastogenesis mostly through production of IL-17 (Fig. 3, A and C). Therefore, the osteoclastogenic ability of Th17 cells does not require cell–cell contact with osteoclast precursor cells, but additional membrane-bound mediators such as RANKL and CD40L may also contribute (46, 47). IL-17 is known to act on the osteoclastogenesis-supporting cells to induce RANKL (25). It should be noted that the effect of IL-17 is not limited to this direct effect on the osteoclastogenesis-supporting cells. IL-17 facilitates local inflammation by recruiting and activating immune cells, which leads to an abundance of inflammatory cytokines such as TNF-α and IL-1 (9, 10). The inflammatory cytokines enhance RANKL expression on osteoclastogenesis-supporting cells and activate osteoclast precursor cells by synergizing with RANKL signaling. A relatively high expression of RANKL on Th17 cells may also participate in the enhanced osteoclastogenesis (Fig. 3 E). Collectively, Th17 cells can be called an osteoclastogenic Th subset not only because Th17 cells have positive effects on osteoclastogenesis in vitro, but also because they tip the balance of the microenvironments in favor of osteoclast differentiation.

It is worth noting that Th17 cells do not induce osteoclastogenesis in the absence of osteoblasts. This strongly suggests that RANKL expressed on Th17 cells alone is not sufficient to induce osteoclastogenesis, although this is partly because even Th17 cells produce a small amount of IFN-γ, which counterbalances the RANKL action. To understand the role of RANKL on T cells in more detail, we need mice of T cell–specific ablation of the *RANKL* gene, which are currently unavailable. But it is conceivable that RANKL expressed on adherent cells such as osteoblasts has more potent effects than that expressed on T cells. This mechanism may also explain why osteoclasts are formed only in the bone microenvironments, but it currently remains to be clarified. We consider the following explanations: (a) T cell expression of membrane-bound RANKL, which is more osteoclastogenic than the soluble form (48), is very low compared with that on osteoblasts; (b) costimulatory signals provided specifically by osteoblasts (12, 27) are missing in T cells; and (c) cell adhesion induces specific signals including those mediated by integrins, which are also important for osteoclastogenesis (49).

In our study, T reg cells had no apparent effect on osteoclastogenesis in vitro (Fig. 1 G). However, their function in the regulation of bone metabolism should be investigated in vivo considering the recent finding that the development of Th17 cells and T reg cells is coordinately regulated (10, 35, 36).

The importance of the IL-23–IL-17 axis in the autoimmune inflammation has been demonstrated in a variety of models of autoimmune diseases such as arthritis and encephalomyelitis (23, 24, 38). In arthritis models, *IL-17*$^{-/-}$ mice were protected from the development of destructive arthritis (24), whereas collagen-induced arthritis is exacerbated in IFN-γ receptor–deficient mice (21, 22). The specific role of IL-23 compared with IL-12 in the development of arthritis has been clearly demonstrated by a genetic study using mice deficient in p19 and p35 (23). Based on these observations, the IL-23–IL-17 axis inducing Th17 cells, rather than the IL-12–IFN-γ axis inducing Th1 cells, is critical for the development of autoimmune arthritis. Our study also provides evidence that the IL-23–IL-17 axis plays a critical role even in a model of bone loss induced by local inflammation that is independent of autoimmunity (Fig. 4 D), suggesting that the IL-23–IL-17 axis is not only essential for the onset phase, but also for the destruction phase of autoimmune arthritis characterized by the T cell–mediated activation of osteoclastogenesis. Thus, Th17 cells, an osteoclastogenic subset, have profound relevance in the bone damage that takes place in autoimmune arthritis. The identification of T cell subsets in the synovium of arthritis is a challenging issue of great importance that should be pursued in a future study. Considering the strong inhibitory effects of Th1 cells on osteoclastogenesis, Th17 cells may be overwhelmingly dominant and the co-localization of Th1 cells is unlikely, at least under the microenvironments in which osteoclastogenesis efficiently occurs. The positive correlation between IL-23 and RANKL expression in the synovium of RA patients further suggests the importance of IL-23 in the regulation of local osteoclastogenesis through IL-17 (Fig. 5 A). Despite the importance of TGF-β and IL-6 in the initiation of Th17 development (10, 35, 36), Th17 cells can be obtained in an IL-23–stimulated culture system without adding exogenous TGF-β/IL-6, suggesting that the endogenous level of TGF-β/IL-6 may suffice for the initiation and that osteoclastogenic activity of Th17 cells is mainly determined by IL-23 under certain pathological conditions.

For the treatment of RA, there are several drugs available, most of which were developed to modulate immune reactions. The antirheumatic drugs are effective in treating pain and inflammation, but patients still fairly frequently have to undergo joint replacement surgery because of the progressive bone damage despite long-term treatment with antirheumatic drugs. Therefore, it is clinically an urgent issue to establish a method to prevent such persistent bone destruction (3). Although rheumatologists are now aware of the great impact that anti-TNF therapy has had on the management of RA (50), it is still not determined whether all patients respond